

**EXAMINATION OF PRIMARY EPITHELIAL
CELLS UNDER NORMAL AND
PATHOPHYSIOLOGICAL CONDITIONS**

Ph.D. Thesis

Viktória Venglovecz

**First Department of Medicine,
University of Szeged,
Szeged, Hungary**

2008

TABLE OF CONTENTS

LIST OF ABBREVIATIONS	2
LIST OF FULL PAPERS CITED IN THE THESIS.....	3
SUMMARY	5
1. INTRODUCTION	7
2. MATERIALS AND METHODS	10
2.1. Solutions and chemicals.....	10
2.2. Animals and experimental protocols	11
2.2.1 Mice	11
2.2.2 Rabbits	11
2.2.3 Guinea pig.....	11
2.2.4 Rats	12
2.3. Ethics	12
2.4. Isolation and culture of primary tissues	12
2.4.1. Isolation of gastric gland.....	12
2.4.2. Isolation of intra/interlobular lacrimal gland ducts.....	13
2.4.3. Isolation of intra/interlobular guinea pig ducts.....	13
2.5. Measurement of intracellular pH and calcium	13
2.6. Microperfusion of pancreatic ducts	14
2.7. Measurement of bicarbonate secretion.....	14
2.8. Measurement of Na ⁺ /HCO ₃ ⁻ cotransporter and Na ⁺ /H ⁺ exchanger activity	15
2.9. Determination of buffering capacity and base flux	15
2.10. Western blotting.....	16
2.11. Transmission electron microscopy	16
2.12. Statistical analysis.....	16
3. RESULTS	17
3.1. Functional characterization of cultured gastric glands	17
3.2. Characterization of the acid/base transporters of the lacrimal gland ductal epithelia ...	19
3.3.1. Morphology of isolated ducts	19
3.3.2. Resting pH _i of the lacrimal gland ductal epithelia.....	19
3.3.3. Na ⁺ /H ⁺ exchanger	20
3.3.4. Na ⁺ /HCO ₃ ⁻ co-transporter.....	20
3.3.5. Cl ⁻ /HCO ₃ ⁻ exchange activity.....	20
3.3.6. pH _i recovery from alkali and acid load.....	21
3.3.7. Ca ²⁺ signaling during parasympathomimetic stimulation	23
3.3.8. The effects of carbachol on the Na ⁺ /H ⁺ and anion exchangers	24
3.3. Differential effect of bile acids on pancreatic ductal cells.....	26
3.3.1. Effect of basolateral exposure to bile acids on duct cell pH _i	26
3.3.2. Effect of luminal exposure to bile acids on duct cell pH _i	28
3.3.3. Recovery of duct cell pH _i during continued exposure to bile acids.....	29
3.3.4. Effect of bile acids on HCO ₃ ⁻ secretion	30
3.3.5. Relationship between the inhibitory and stimulatory effects of chenodeoxycholate on HCO ₃ ⁻ secretion and chenodeoxycholate-induced changes in [Ca ²⁺] _i	33
3.4. The influence of hyperlipidemia on pancreatic HSP72 and IκB-α expression in acute necrotizing pancreatitis	34
4. DISCUSSION	35
5. ACKNOWLEDGEMENTS	42
6. REFERENCES.....	44
7. ANNEX	53

LIST OF ABBREVIATIONS

Arg	Arginine
Ach	Acetylcholine
AE	Cl ⁻ /HCO ₃ ⁻ exchanger
BAPTA-AM	1,2-bis(o-aminophenoxy)ethane-N,N,N',N'-tetraacetic acid
BCECF-AM	2.7-bis-(2-carboxyethyl)-5-(and-6-)carboxyfluorescein acetoxymethyl ester
CACC	Calcium-activated chloride channel
[Ca²⁺]_i	Intracellular calcium concentration
CDC	Chenodeoxycholate
CFTR	Cystic fibrosis transmembrane conductance regulator
DMSO	Dimethyl sulfoxide
ECL	Enterochromaffin-like cell
FBS	Fetal bovine serum
FURA 2-AM	5-Oxazolecarboxylic acid, 2-(6-(bis(carboxymethyl)amino)-5-(2-(2-(bis(carboxymethyl)amino)-5-methylphenoxy)ethoxy)-2-benzofuranyl)-5-oxazolecarboxylic acetoxymethyl ester
G17	Heptadecapeptide gastrin
Gas-KO	Gastrin null
GCDC	Glycochenodeoxycholate
HBSS	Hank's balanced salts solution
H₂DIDS	Dihydro-4,4'-diisothiocyanostilbene-2,2'-disulfonic acid
HSP72	Heat shock protein 72
IκBs	Inhibitor of κB proteins
LCDC	Lacrimal gland ductal cell
NBC	Na ⁺ /HCO ₃ ⁻ cotransporter
NHE	Na ⁺ /H ⁺ exchanger
NF-κB	Nuclear factor κB
OATP	Organic anion transporter protein
pH_i	Intracellular pH
PPDC	Primary pancreatic ductal cells
ROI	Region of interest

LIST OF FULL PAPERS CITED IN THE THESIS

I. Pagliocca A., Hegyi P., **Venglovecz V.**, Rackstraw S.A., Khan Z., Wang T.C., Dimaline R., Varró A., Dockray G.J. Identification of ezrin as target of gastrin in immature gastric parietal cells. *J Physiol* (under revision). **IF: 4.407**

II. Tóth-Molnár E., **Venglovecz V.**, Ózsvári B., Rakonczay Z. Jr., Varró A., Papp J.G., Tóth A., Lonovics J., Takács T., Ignáth I., Iványi B., Hegyi P. New experimental method to study acid/base transporters and their regulation in lacrimal gland ductal epithelia. *Invest Ophthalmol Vis Sci* 2007;**48**:3746-3755. **Please note:** the first two authors equally contributed to this work (mentioned in the article), therefore, both of them have to be regarded as first authors. **IF: 3.643**

III. **Venglovecz V.**, Rakonczay Z. Jr., Ózsvári B., Takács T., Lonovics J., Varró A., Gray M.A., Argent B.E., Hegyi P. Effects of bile acids on pancreatic ductal bicarbonate secretion in guinea pig. *Gut* (under final revision). **IF: 9.02**

IV. Czakó L., Szabolcs A., Vajda Á., Csáti S., **Venglovecz V.**, Rakonczay Z. Jr., Hegyi P., Tizslavicz L., Csont T., Pósa A., Berkó A., Varga Cs., Varga I.S., Boros I., Lonovics J. Hyperlipidemia induced by a cholesterol-rich diet aggravates necrotizing pancreatitis in rats. *Eur J Pharmacol* 2007;**572**:74-81. **IF: 2.477**

LIST OF FULL PAPERS RELATED TO THE SUBJECT OF THE THESIS

V. Hegyi P., Rakonczay Z., Farkas K., **Venglovecz V.**, Ózsvári B., Seidler U., Gray M.A., Argent B.E. Controversies in the role of SLC26 anion exchangers in pancreatic ductal bicarbonate secretion. *Pancreas*, 07-00649, (accepted). **IF: 2.12**

Number of full publications:	5
Cumulative impact factor:	21.667
Number of abstract publications:	15
Number of scientific presentations:	16

SUMMARY

Background & Aims. Epithelial cells play an important role in several processes, including protection, absorption or secretion. Secretory epithelia of exocrine glands are responsible for the transport of acid, base and electrolytes, therefore play an essential role in the regulation of the volume and ion composition of body fluids. Since most of the epithelial diseases result from incomplete fluid secretion or absorption, the exact knowledge of epithelial ion transport processes are of crucial importance. In most of the exocrine glands, the epithelial function and regulation is not completely understood. The **aim** of my work was to investigate the ion transport mechanisms of i) gastric parietal cells, ii) lacrimal intra/interlobular ducts and iii) pancreatic intra/interlobular ducts under normal [Annex No. I-II] and pathophysiological conditions [Annex No. III]. In addition, we investigated the role of hyperlipidemia in acute pancreatitis, with a particular emphasis on the expression of pancreatic heat shock protein 72 (HSP72) and inhibitor of κ B proteins (IkBs) [Annex No. IV].

i) It is generally known that gastrin has a central role in the regulation of acid secretion by parietal cells. However, the role of gastrin in the maturation of parietal cell function is not fully understood.

ii) Similarly to the gastric gland, not much data is available concerning the regulatory mechanisms of the lacrimal gland ductal cells (LGDC). Studies have been conducted that investigate the mixed fluid and protein secretion of isolated lacrimal acini, but no methods have been developed to characterize LGDC secretion.

iii) Nevertheless, the examination of the function of exocrine glands is very important not only under normal but pathophysiological conditions, since numerous protective mechanisms can only be investigated under abnormal conditions. One of the most common diseases which is related to exocrine glands is acute pancreatitis. Biliary reflux or hyperlipidemia are well known etiologic factors which are associated with acute pancreatitis or aggravate its course. However our knowledge concerning the protective mechanisms during acute pancreatitis is limited.

Methods. We performed our experiments on isolated primary epithelial cells. ^(see annex No. I-III)

During the isolation process the epithelial cells retained their polarity and functional characteristics, thus they were suitable to study their transport properties. The activity of the ion transporters were investigated using a fluorescent dye BCECF to monitor intracellular pH (pH_i) by microfluorimetry. The intracellular calcium concentration ($[\text{Ca}^{2+}]_i$) was measured by FURA-2. In addition, we performed western blots to investigate the effect of hyperlipidemia

on the expression of pancreatic HSP72 and I κ Bs in rats with acute necrotizing pancreatitis. Acute pancreatitis was induced with 2x2 g/kg body weight of L-arginine (Arg) respectively, in normal and hyperlipidemic rats. (see annex No. IV.)

Results and Conclusions. i) In gastrin null mice (Gas-KO mice) acute gastrin stimulation (incubation for 1 hr *in vitro* with 1 nM heptadecapeptide gastrin (G17) did not restore H⁺ pump activity in gastric parietal cells, however, prolonged exposure to gastrin (incubation for 24 hr *in vitro* with 1 nM G17, which we refer to as “priming”) totally restored H⁺ secretion. Our results suggest, that gastrin is a key factor in parietal cell maturation and is required for acid secretion.

ii) The next part of this thesis focuses on the basic transport mechanisms of the lacrimal gland ductal epithelia. In this study, we have developed a rapid method to isolate intact rabbit lacrimal gland ducts, which allowed us for the first time to perform real-time functional experiments on cleaned ducts. Our results showed that LGDC express functionally active Na⁺/H⁺ (NHEs), and Cl⁻/HCO₃⁻ exchangers (AEs). Moreover, parasympathomimetic stimulation by carbachol stimulated the NHE and AE, via elevation of intracellular calcium concentration. These data combined with the novel isolation facilitated understanding of the regulation mechanisms of ductal cell secretion at cellular and molecular levels.

iii) In the pathophysiological studies, in connection with the defence mechanisms during biliary pancreatitis, we have shown that luminal administration of a low dose (0.1mM) of chenodeoxycholate (CDC) stimulated HCO₃⁻ secretion, while a high dose (1mM) of this bile acid, both from the luminal and basolateral membrane, inhibited HCO₃⁻ secretion. We have also shown that 1,2-bis(o-aminophenoxy)ethane-N,N,N',N'-tetraacetic acid (BAPTA-AM) blocked the stimulatory effect of low doses of CDC on HCO₃⁻ secretion, but did not modulate the inhibitory effect of high doses of CDC. Our hypothesis is that this stimulated HCO₃⁻ secretion by low concentration of CDC acts to protect the pancreas against toxic bile, whereas the inhibition of HCO₃⁻ secretion by high concentrations of bile acids may contribute to the progression of acute pancreatitis.

Finally, we have found that the pancreatic HSP72 expression during acute pancreatitis was not influenced by hyperlipidemia, however the level of I κ B- α was significantly lower in pancreatic rats on cholesterol enriched diet as compared with those on normal diet.

In summary in this thesis we tried to provide a better understanding of epithelial cell function under normal and pathophysiological conditions. Our results may open up the possibility to develop new strategies in the treatment of diseases.

1. INTRODUCTION

Normal epithelial ion transport is essential for the maintenance of healthy function of several exocrine glands. For example, in the pancreas it helps to wash out the digestive enzymes,^[1] while the acid secretion by the stomach protects against infection by pathogenic micro-organisms.^[2-3] The fluid secretory properties of exocrine glands are mainly due to the epithelial cells. The epithelial cells are usually organized into a branching ductal system, which form the structural frame of numerous glands, such as the pancreas^[4] or the lacrimal gland.^[5, 6] Due to this tubular arrangement, luminal and basolateral „sides” can be distinguished on epithelial cells. The two membranes express different sets of transport proteins which result in the polarity of the epithelial tissue.^[7] The polarized feature of these cells ensures the vectorial transport of the ions and water from the basolateral membrane to the lumen. This fluid secretion is a complex process and is highly regulated by both hormonal and neuronal mechanisms. Despite of the fact that epithelial cells play an important role in the maintenance of a standard environment, our knowledge of epithelial function is incomplete, especially in certain diseases, such as acute pancreatitis or dry eye syndrome. The general goal of our studies summarized in this thesis was to investigate the secretory mechanisms and intracellular regulation of various exocrine glands (especially the gastric gland, the lacrimal gland, and the pancreas) in normal and pathophysiological conditions. The better understanding of the mechanisms of epithelial ion transport processes may help us to develop drugs in the treatment of different diseases.

Research on gastric epithelial cell physiology has mainly focused on the role of gastrin in the regulation of acid secretion in parietal cell maturation. Several lines of evidence indicate that the gastric hormone gastrin is a potent stimulator of gastric acid secretion.^[8, 9] It is well established that in addition to CCK-2 receptors, parietal cells also express H₂ histamine receptors and M₃ muscarinic receptors.^[10] Activation of each of these receptors is associated with parietal cell stimulation.^[11] However, physiologically it is generally thought that gastrin acts primarily through release of histamine from enterochromaffin-like (ECL) cells, which then acts as a paracrine regulator of parietal cell function.^[12] Studies in Gas-KO mice suggest that gastrin is involved in more than just the acute regulation of acid secretion. In these animals, parietal cells occur predominantly in an immature form so that they secrete little acid and are refractory to acute administration of gastrin, histamine or the muscarinic agonist carbachol.^[13, 14] Interestingly, administration of gastrin over a period of a few days

induces acid secretion, and the capacity to respond to the main secretagogues,^[14, 15] suggesting that in addition to its role in stimulating acid secretory responses during digestion, gastrin also plays a role in regulating the final steps of parietal cell maturation. The main focus of this study was to investigate the role of gastrin both in acid secretion and in parietal cell maturation demonstrated by H⁺/K⁺ ATPase activity.

The secretory properties of epithelial cells was not only investigated in gastric glands, but also in the lacrimal gland. In the lacrimal gland one of the main cell types is the ductal cell.^[5, 6] The lacrimal gland ductal cells have a major role in fluid secretion which are essential in maintaining a healthy, normal function of the ocular surface. When tear secretion decreases in amount or changes in composition, dry eye syndrome (keratoconjunctivitis sicca) can develop and in the worst case can induce corneal ulceration and vascularisation leading to serious visual impairment.^[16, 17] Most of the available methods to study protein and fluid secretion of lacrimal gland are focused on acinar cells,^[18, 19] however much less is known about the LGDC.^[20, 21] Ubels et al. have recently described a laser capture microdissection technique for cDNA microarray analysis and immunohistochemistry using frozen lacrimal gland,^[21] however, no methods have been developed to characterize the LGDC secretion in viable ductal cells. Nevertheless, the secretory mechanisms of the ductal epithelia may play a physiological role in the maintenance of the standard environment of the cornea and the conjunctiva. In this part of my studies, our aim was to develop a method to isolate lacrimal ducts, in order to open up the possibility to obtain more information on the regulation of lacrimal gland epithelial tissue and to characterize LGDC acid/base ion transporters mediating fluid secretion.

We were interested in epithelial function not only under normal but also under pathophysiological conditions. Most of the pathophysiological investigations focus on the damaging factors, which alter the course of several diseases. For example in the pancreas a several factors have been shown to aggravate acute pancreatitis,^[22, 23] however, the role of protective mechanisms are relatively less understood. Since acute pancreatitis is associated with high morbidity and mortality our aim was to investigate which are those defensive mechanisms that may interfere with the aggravation of this disease. The pancreatic fluid hypersecretion during acute pancreatitis may be such a protective effect against pancreatic injury. The basal fluid secretion of the pancreas is responsible for washing out the digestive enzymes into the duodenum, and it contributes to the neutralization of the acid chyme entering the duodenum from the stomach.^[1] The main transporters which are involved in this secretion across the luminal membrane are the Cl⁻/HCO₃⁻ exchanger (luminal AE) and the

cAMP-activated cystic fibrosis transmembrane conductance regulator (CFTR).^[24-27] It has been shown that this fluid secretion can increase in certain conditions,^[28, 29] but the protective effect of this hypersecretion is poorly investigated.^[30] We believe that the increased secretion is mainly due to pancreatic ductal epithelial cells, which may represent a defence mechanism against toxic factors. Since refluxed bile is one of the most common cause in the development of acute pancreatitis,^[31-34] we investigated the effect of bile acids on pancreatic ductal HCO_3^- secretion. The pathogenesis underlying the development of acute biliary pancreatitis is not well understood. Although the bile can reach both acinar and ductal cells during biliary pancreatitis, much more research has been done on acinar cells.^[35-38] To date, scientists have mostly examined the permeability and morphology of ductal cells following the administration of bile acids.^[39-41] It has been shown that the permeability of the pancreatic ductal epithelium to HCO_3^- and Cl^- is increased by exposure to various bile salts at concentrations within the range normally found in the duodenum.^[41] Although one of the main functions of the pancreatic ductal epithelium is to secrete the HCO_3^- ions found in pancreatic juice,^[42, 43] no data are available on the effects of bile acids on HCO_3^- secretion. However, it has been shown, that retrograde injection of sodium taurocholate into the rat pancreatic duct induces fluid hypersecretion and decreases protein output in the initial phase of acute pancreatitis.^[44] Our hypothesis is that the hypersecretory effect of bile acids, may represents a defence mechanism in order to avoid pancreatic injury. We planned in this study to characterize the effects of bile acids on ductal iontransport processes, especially on HCO_3^- secretion. We performed our experiments on intact isolated guinea pig pancreatic ducts, because the guinea pig pancreas secretes a juice containing ~140mM NaHCO_3 as does the human gland.^[45]

Hyperlipidemia is also associated with acute pancreatitis,^[46] however, the role of hyperlipidemia in the pathogenesis of acute pancreatitis is uncertain. Recent evidence indicates that a high-cholesterol diet alters the expression of HSP72 and the activation of nuclear factor κB (NF- κB).^[47, 48] NF- κB plays a critical role in the pathogenesis of acute experimental pancreatitis by regulating the expressions of many proinflammatory genes.^[49, 50] The possible protective factors during hyperlipidemic acute pancreatitis are unknown. Since it is well known that the accumulation of the highly stress-inducible member of the HSP72 in response to a variety of stressors confers long-lasting protection against further stress injury,^[49, 50] we investigated whether hyperlipidemia alters the pancreatic heat stress response. In addition we examined the expression of $\text{I}\kappa\text{B}-\alpha$, the inhibitor protein of NF- κB ,^[51] during hyperlipidemic acute pancreatitis.

2. MATERIALS AND METHODS

2.1. Solutions and chemicals

The compositions of the solutions used are shown in Table 1. HEPES-buffered solutions were gassed with 100% O₂ and their pH was set to 7.4 with NaOH or HCl at 37°C. HCO₃⁻-buffered solutions were gassed with 95% O₂ / 5% CO₂ to set pH to 7.4 at 37°C. Chromatographically pure collagenase was purchased from Worthington (Lakewood, NJ, USA). CellTak was obtained from Becton Dickinson Labware (Bedford, MA, USA). 2.7-bis-(2-carboxyethyl)-5-(and-6-)carboxyfluorescein, acetoxymethyl ester (BCECF-AM), 5-Oxazolecarboxylic, 2-(6-(bis(carboxymethyl)amino)-5-(2-(2-(bis(carboxymethyl)amino)-5-methylphenoxy)ethoxy)-2-benzofuranyl)-5-oxazolecarboxylic acetoxymethyl ester (FURA 2-AM), dyhydro-4,4'-diisothiocyanostilbene-2,2'-disulfonic acid (H₂DIDS) and 1,2-bis(o-aminophenoxy)ethane-N,N,N',N'-tetraacetic acid (BAPTA-AM) were from Molecular Probes Inc. (Eugene, OR, USA). Nigericin was dissolved in absolute ethanol and amiloride in DMSO. COOH-terminally amidated, unsulphated, G17 was obtained from Bachem (St Helens, Merseyside, UK). Omeprazole was kindly donated by Astra Zeneca (London, U.K.). The rabbit anti-HSP72 antibody was a generous gift from Dr. István Kurucz (IVAX Drug Research Institute, Budapest, Hungary). The rabbit anti-IκB-α was purchased from Santa Cruz Biotechnology (Santa Cruz, CA, USA). The goat horseradish peroxidase conjugated anti-rabbit secondary antibody was from DAKO (Glostrup, Denmark). Bile acids and all other chemicals were obtained from Sigma-Aldrich (Budapest, Hungary).

Table 1. Composition of solutions.

	Standard HEPES	Standard HCO ₃ ⁻	High-K ⁺ HEPES	NH ₄ ⁺ in HEPES	NH ₄ ⁺ in HCO ₃ ⁻	Na ⁺ -free HEPES	Na ⁺ -free HCO ₃ ⁻	Cl ⁻ -free HEPES	Cl ⁻ -free HCO ₃ ⁻	Ca ²⁺ -free HEPES
NaCl	130	115	5	110	95					132
KCl	5	5	130	5	5	5	5			5
MgCl ₂	1	1	1	1	1	1	1			1
CaCl ₂	1	1	1	1	1	1	1			
Na-HEPES	10		10	10						10
Glucose	10	10	10	10	10	10	10	10	10	10
NaHCO ₃		25			25			25	25	
NH ₄ Cl				20	20					
HEPES						10				
NMDG-Cl						140	115			
Choline-HCO ₃ ⁻							25			
Atropine							0.01			
Na-gluconate								140	115	
Mg-gluconate								1	1	
Ca-gluconate								6	6	
KH ₂ -sulfate								5	5	

Values are concentrations in mM.

2.2. Animals and experimental protocols

2.2.1 Mice

We used mice in order to examine the priming effect of gastrin on gastrin knock-out parietal cells.

Gas-KO mice on a C57Bl/6 background have been described previously.^[13] Mice were housed in polycarbonate-bottomed cages with a strict light cycle (lights on at 0700 and off at 1900) and fed on a commercial pellet diet (LATI, Gödöllő, Hungary) and water. The mice (10-12 weeks) were killed by standard carbon dioxide asphyxiation followed by cervical dislocation and then the stomach was rapidly removed. Approximately half of the non-secretory epithelium was removed, the pyloric sphincter was then directed through the newly created fundic opening and the stomach everted and sealed by ligation of the remaining non-secretory epithelium.

2.2.2 Rabbits

We used rabbits in order to characterize the acid/base ion transporters of lacrimal gland ductal cells.

Adult male New Zealand white rabbits weighing 2-2.5 kg were sedated with 50 mg/kg pentobarbital and humanely killed by cervical dislocation. The superotemporal and inferotemporal portions of the conjunctival fornices were dissected after wide temporal canthotomy. The eyeball was then dislocated inferonasally and the temporal part of the orbital connective tissues were excised using stereomicroscope. The preparation procedure revealed the main lobes of the lacrimal gland under the roof of the orbit, which were removed by gentle pressure with forceps and final separation with scissors. Both intraorbital lacrimal glands were carefully dissected.

2.2.3 Guinea pig

We used guinea pigs in order to examine the effect of bile acids on pancreatic ductal bicarbonate secretion.

Guinea pigs weighing 150-250g were kept at a constant room temperature of 22 ± 2 °C, under 12-h light-dark cycles, and were allowed free access to water and standard laboratory chow. Guinea pigs were killed humanly by cervical dislocation, and then the pancreas was removed.

2.2.4 Rats

We used rats in order to investigate the role of hyperlipidemia in the pathogenesis of acute pancreatitis.

Wistar rats weighing 80-100 g were kept at a constant room temperature of 22 ± 2 °C, under 12-h light-dark cycles, and were fed laboratory chow enriched with 3% cholesterol (cholesterol group) or standard chow (LATI, Gödöllő, Hungary) (control group) for 16 weeks. We used a necrotizing pancreatitis model to induce experimental pancreatitis.^[52, 53]

At the end of this 16-week controlled-diet period, acute necrotizing pancreatitis was induced with 2×2 g/kg body weight of arginine (Arg) intraperitoneally in separate groups of normal and hyperlipidemic rats (Arg and cholesterol+Arg groups).^[54-56] The control rats received 8.6% glycine in 0.9% physiological saline at the same times instead of Arg. 24 h after the first Arg injection, the rats were sacrificed by exsanguination through the abdominal aorta. The pancreas was quickly removed, cleaned from fat and lymph nodes, weighed, and frozen in liquid nitrogen and stored at -80 °C until use.

Akut nekrotizáló pankreatitist 2 g/2 kg testsúly dózisú arginin intraperitoneális adásával váltottunk ki, mind a kontrol mind pedig a koleszterinben gazdag diétán tartott állatokban.

2.3. Ethics

The experiments were conducted in compliance with the *Guide for the Care and Use of Laboratory Animals* (U.S.A. NIH publication No 85-23, revised 1985). In addition, the experimental protocols were approved by the local Ethical Board of the University of Szeged, Hungary.

2.4. Isolation and culture of primary tissues

2.4.1. Isolation of gastric gland

Stomachs were washed in ice-cold Hanks' balanced salt solution (HBSS) and were filled by injection via a 23-gauge needle with 0.5 ml of $0.5 \text{ mg}\cdot\text{ml}^{-1}$ collagenase A (Roche Molecular Biochemicals, East Sussex, UK). Using a modification of a previously described method,^[57] glands were obtained by washing the stomach in pre-warmed (37°C) HBSS (3 times), followed by incubation in dithiothreitol (5 ml, 1 mM) for 15 minutes, washing again in

HBSS (3 times), and finally incubating in collagenase A (7.5 ml, 0.32 mg ml⁻¹, 30 minutes, 37°C) in an atmosphere of 95%O₂/5%CO₂ with shaking at 100 cycles per minute. Rupturing of the inverted stomach generally indicated adequate digestion to yield isolated glands. At this stage tissue was triturated using a wide mouthed plastic pipette, larger fragments were allowed to settle under gravity (45 seconds), leaving the isolated glands in suspension.^[58] The supernatant containing isolated glands was then transferred to a clean tube, shaken to release additional glands, allowed to settle under gravity for 45 minutes on ice and the supernatant discarded. The isolated gastric glands from one mouse were suspended in 1.0 ml Dulbecco's Modified Eagle's Medium supplemented with 10% fetal bovine serum (FBS) and 1% antibiotic-antimycotic solution and cultured at 37°C in a humidified atmosphere of 95%O₂/5%CO₂. Medium was changed after 24 hours and experiments started 24 hours later. Two protocols were used: (1) For "priming", glands were incubated for 24 hours in medium containing G17 (1.0 nM). (2) For "acute" stimulation, glands were incubated for 1 hour with G17 or other drugs as appropriate. Typically, after priming glands were either incubated with an acute stimulant or with control medium.

2.4.2. Isolation of intra/interlobular lacrimal gland ducts

The isolation of the intra/interlobular ducts was similar to that described for the pancreas,^[59] except that the isolation solution did not contain trypsin inhibitor.

2.4.3. Isolation of intra/interlobular guinea pig ducts

Intra/interlobular ducts were isolated by enzymatic digestion and microdissection as described previously.^[59] The ducts were cultured overnight in a 37 °C incubator gassed with 5 % CO₂/95 % air. During the overnight incubation, both ends of the isolated ducts seal to form a closed sac that swells due to accumulation of secretion in the duct lumen.

2.5. Measurement of intracellular pH and calcium

Intracellular pH (pH_i) was estimated using the pH-sensitive fluorescent dye BCECF-AM. The gastric glands were cultured on coverslips (24mm), the pancreatic and lacrimal gland ducts were attached (using Cell Tak) to coverslips (24mm), which formed the base of a perfusion chamber mounted on a microscope (Olympus, Budapest, Hungary). The tissues were bathed in standard Hepes solution at 37 °C and loaded with the membrane permeable acetoxymethyl derivative of BCECF (2 μmol/L) for 20-30 min. After loading, the tissues were continuously perfused with solutions at a rate of 5-6 mL/min. pH_i was measured using a

Cell^R imaging system (Olympus, Budapest, Hungary). 4-5 small areas (Region of interests – ROIs) of 5-10 cells in each intact duct were excited with light at wavelengths of 490 and 440 nm, and the 490/440 fluorescence emission ratio was measured at 535 nm. One pH_i measurement was obtained per second. *In situ* calibration of the fluorescence signal was performed using the high K⁺-nigericin technique.^[60, 61]

Measurement of [Ca²⁺]_i was performed using the same method except that the cells were loaded with the Ca²⁺-sensitive fluorescent dye FURA 2-AM (5 μmol/L) for 60 min. For excitation, 340 and 380 nm filters were used, and the changes in [Ca²⁺]_i were calculated from the fluorescence ratio (F₃₄₀/F₃₈₀) measured at 510 nm.

2.6. Microperfusion of pancreatic ducts

The lumen of the cultured pancreatic ducts was microperfused using a modification of the method described by Ishiguro et al.^[62] Two concentric pipettes were used for the microperfusion. One end of a sealed duct was cut off and the other end was aspirated into the outer, holding pipette, then the inner, perfusion pipette, was gently inserted into the lumen while a negative pressure was applied to the holding pipette using a syringe. The duct was then perfused at a rate of 10-30 μl/min, the luminal perfusate left the duct at the open end. The high rate of the bath perfusion (5-6 mL/min), which was in the same direction as the flow of luminal perfusate, ensured that the outgoing luminal perfusate did not gain access to the basolateral surface of the duct cells. Replacement of the luminal perfusate took up to 2 minutes.

2.7. Measurement of bicarbonate secretion

We utilized three methods to determine the HCO₃⁻ efflux across the luminal membrane.

In the inhibitory stop method, the basolateral Na⁺/HCO₃⁻ cotransporter (NBC) and the Na⁺/H⁺ exchanger (NHE) were blocked using H₂DIDS (0.5 mM) and amiloride (0.2 mM) for 3 min administered from the basolateral side. The inhibition of these transporters caused a marked decrease in pH_i. The rate of pH_i acidification after the exposure to H₂DIDS and amiloride reflects the intracellular buffering capacity and the rate at which HCO₃⁻ effluxes (i.e. is secreted) across the apical membrane via Cl⁻/HCO₃⁻ exchangers and possibly CFTR.^[63, 64] The initial rate of intracellular acidification (dpH/dt), over the first 60 seconds was

calculated by linear regression analysis using 60 data points (one pH_i measurements per second).

In the alkali load method, HCO_3^- secretion was estimated by the rate of pH_i recovery from an alkaline load. In these experiments ducts were exposed to 20 mM NH_4Cl in $\text{HCO}_3^-/\text{CO}_2$ -buffered solution from the basolateral side which produced an immediate increase in pH_i due to the rapid influx of NH_3 across the membrane. After the alkalisation there was a recovery in pH_i toward the basal value. Recently, we demonstrated that recovery of pH_i under these conditions was dependent on the presence of HCO_3^- in the bathing solution, suggesting that it results from HCO_3^- efflux (i.e. secretion) from the duct cells.^[63] In the present study, the initial rate of recovery from alkalosis (dpH/dt) over the first 30 seconds (30 pH_i measurements) in the continued presence of NH_4Cl was calculated as described previously.^[63]

In the Cl^- withdrawal technique, HCO_3^- secretion was characterized by the rate of pH_i elevation (alkalinization) after luminal Cl^- withdrawal.

2.8. Measurement of $\text{Na}^+/\text{HCO}_3^-$ cotransporter and Na^+/H^+ exchanger activity

In the alkali load method, after the removal of NH_4Cl , there is a rapid decrease in pH_i , due to the diffusion of NH_3 out of the cell and the release of H^+ . The recovery from this acid load mostly depends on the activity of NBC and NHE.^[63] In order to study the transporters separately, the experiments were performed in the absence or presence of HCO_3^- . The initial rate of recovery (dpH/dt) over the first 60 seconds (60 pH_i measurements) was calculated as described previously.^[63]

2.9. Determination of buffering capacity and base flux

The total buffering capacity (β_{total}) of the pancreatic duct cells was estimated according to the NH_4^+ pre-pulse technique.^[63, 65] Pancreatic duct cells were exposed to various concentrations of NH_4Cl in Na^+ and HCO_3^- -free solution. β_i (which refers to the ability of intrinsic cellular components to buffer changes of pH_i) was estimated by the Henderson-Hasselbach equation. β_{total} was calculated from: $\beta_{\text{total}} = \beta_i + \beta_{\text{HCO}_3^-} = \beta_i + 2.3 \times [\text{HCO}_3^-]_i$, where $\beta_{\text{HCO}_3^-}$ is the buffering capacity of the $\text{HCO}_3^-/\text{CO}_2$ system. The rates of pH_i change measured in the inhibitor stop, alkali and acid load experiments were converted to transmembrane base flux $J(\text{B}^-)$ using the equation: $J(\text{B}^-) = \text{dpH}/\text{dt} \times \beta_{\text{total}}$. We denoted base influx as $J(\text{B}^-)$ and base efflux (secretion) as $-J(\text{B}^-)$.

2.10. Western blotting

Western blot analysis of pancreatic HSP72 and I κ B- α expression was performed from the cytosolic fraction of the pancreas homogenate as described previously.^[49, 50, 66] Pancreatic tissue was homogenized and diluted to load 40 μ g of total protein on an 8-10 % polyacrylamide gel. After separation by electrophoresis, the proteins were blotted onto a nitrocellulose membrane. After blocking with 5% dry milk, the membranes were incubated with rabbit anti-HSP72 (1:2500 dilution, 60 min), or rabbit anti-I κ B- α (1:500 dilution, 60 min) and with goat antirabbit secondary antibody for 60 min (1:1000). Bands were visualized by enhanced chemiluminescence (ECL Plus; GE Healthcare, Little Chalfont, Buckinghamshire, UK). Thereafter, they were scanned and quantified by using the ImageJ software (NHI, Bethesda, MD, USA). The band densities of the proteins were determined and summed in order to estimate the total level of nitrated proteins. Results are expressed in arbitrary units.

2.11. Transmission electron microscopy

For the electron microscopic studies, the ducts were fixed in 2.5% glutaraldehyde immediately following isolation. The samples were then post-fixed in 1 % osmium tetroxide, dehydrated in a series of graded ethanols, and subsequently embedded in epoxy resin. Ultrathin sections were contrasted with uranyl acetate and lead citrate. Tissue sections were analysed using a Philips CM10 transmission electron microscope.

2.12. Statistical analysis

Results are expressed as means \pm S.E.M. Experiments were evaluated statistically with analysis of variance (ANOVA). P values \leq 0.05 were accepted as significantly significant.

3. RESULTS

3.1. Functional characterization of cultured gastric glands

In order to establish whether there are functional differences between wild-type and Gas-KO parietal cells in cultured glands we monitored pH_i . Parietal cells were identified by lectin staining before the experiments. The resting pH_i of wild-type parietal cells was 7.33 ± 0.02 ($n=10$) and was not significantly different in Gas-KO cells (7.30 ± 0.05). Removal of Na^+ from the standard Hepes solution caused a rapid and marked intracellular acidosis due to the inhibition of NHE activity (Fig. 1A). Exposure to 20 mM NH_4Cl induced an immediate rise in pH_i due to the rapid entry of NH_3 into the cells and its removal produced a rapid decrease in pH_i followed by a slower recovery due to activation of pH_i regulatory mechanisms. In the absence of Na^+ and HCO_3^- , the functionally active acid/base transporter/pump in these circumstances is the H^+/K^+ -ATPase and the initial rate of recovery from acidosis reflects its activity. When 10-1000 pM G17 was included in the medium, there was a concentration-dependent stimulation of pH_i recovery after NH_4Cl due to the stimulated H^+ efflux (Fig. 1B) that was blocked by 100 μM omeprazole indicating that it was attributable to H^+/K^+ ATPase activity (Fig. 1C). The H_2 receptor antagonist ranitidine inhibited the response to 100 pM G17 (which is just above the physiological concentration in plasma), but only partially inhibited the effect of 1 nM G17 consistent with the idea that at physiological concentrations gastrin acts on parietal cells via histamine release from ECL cells, but can act directly at higher concentrations (Fig. 1D). Importantly, in Gas-KO mice the initial recovery of pH_i was significantly decreased compared with wild-type mice (Gas-KO, $0,0054 \pm 0,001$ U/min; wild type, $0,015 \pm 0,002$, $p<0.05$) and was completely refractory to 1 nM G17. However, priming with 1 nM G17, followed by a 2h wash-out period before the experiments, induced the capacity for an acute response to G17 (Fig. 1E).

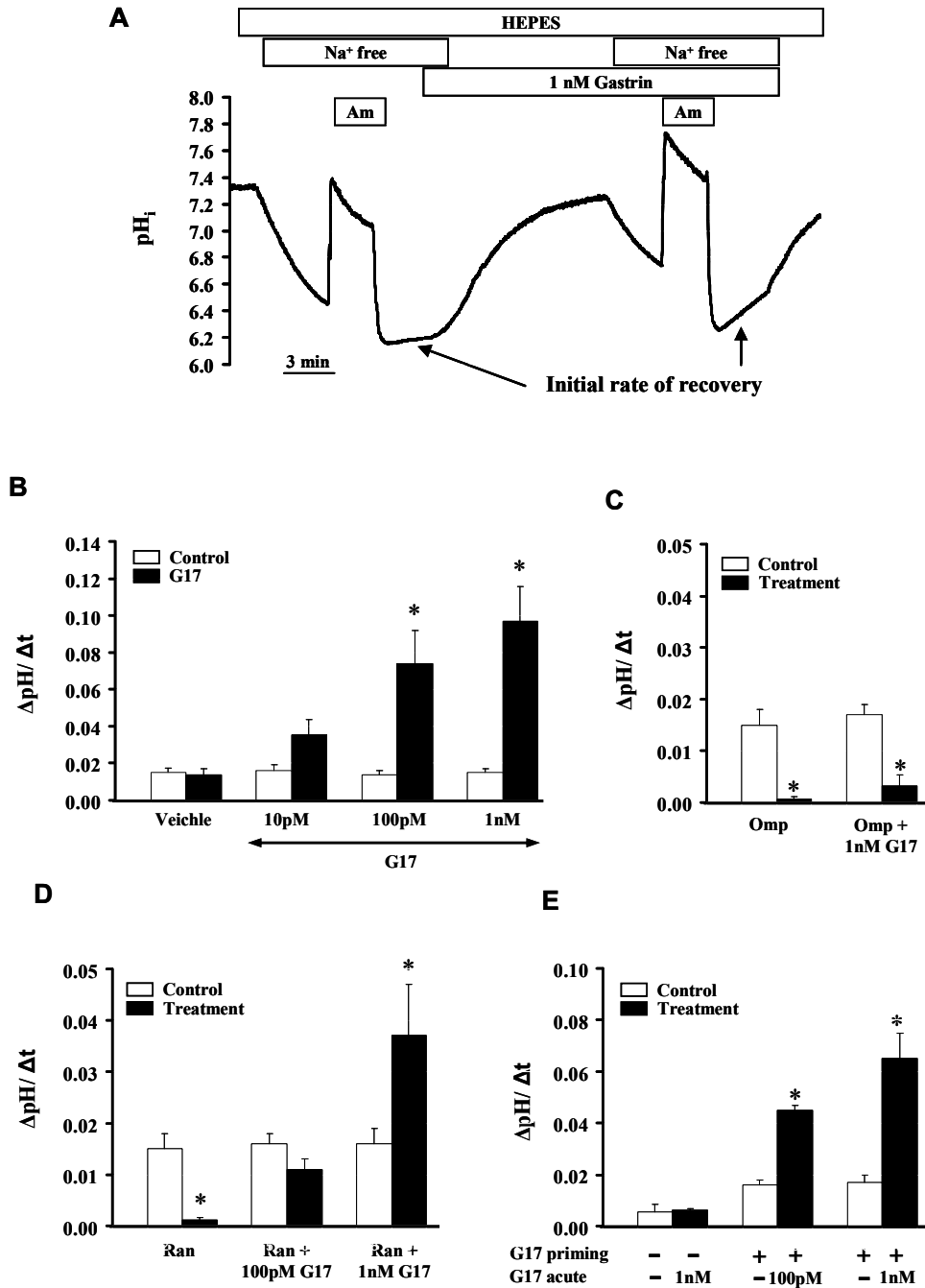


Figure 1. Functional characterisation of parietal cells in cultured gastric glands of Gas-KO and wild type mice. **A**, Representative pH_i trace of gastric gland parietal cells that were twice exposed to 3 min pulses of 20 mM NH₄Cl (Am) in a Na⁺ free HEPES solution, the first exposure being the control and the second the test. The initial rates of pH_i recovery from the acid load (over the first 60sec) were determined for each exposure. G17 was administered for 20 minutes before and during the test exposure and the inhibitors (omeprazole or ranitidine, when used) were administered for 10 minutes between the measurements. **B**, Bar chart shows the summary of the results obtained using ammonium chloride pulses described above. Initial rates of pH_i recovery are shown by the open bars, compared with recovery in the test period (filled bars). Increasing concentrations of G17 stimulated the pH_i recovery after NH₄Cl pulses compatible with increased activity of H⁺/K⁺ ATPase. **C**, the proton pump inhibitor omeprazole (100 μM) completely blocked both unstimulated and G17-stimulated pH_i recovery. **D**, the H₂ receptor antagonist ranitidine (100 μM) inhibited pH_i recovery in response to a low concentration of G17, that could be overcome by higher concentrations of G17. **E**, in parietal cells from GAS-KO mice, incubation *in vitro* with gastrin (1nM, 24 h; “G17 priming”) restored proton pump activity. Means ± SEM for groups of 3 glands/10-15 parietal cells are shown. * p<0.05.

3.2. Characterization of the acid/base transporters of the lacrimal gland ductal epithelia

3.3.1. Morphology of isolated ducts

The ultrastructural examination revealed that small ducts were characterized by numerous microvilli in the apical region, tight junctions, secretory granules, mitochondria and basolateral infoldings (interdigitations) of the cell membrane and basement membrane in the basal region. The cells were relatively rich in vesicles and secretory granules (Fig. 2).

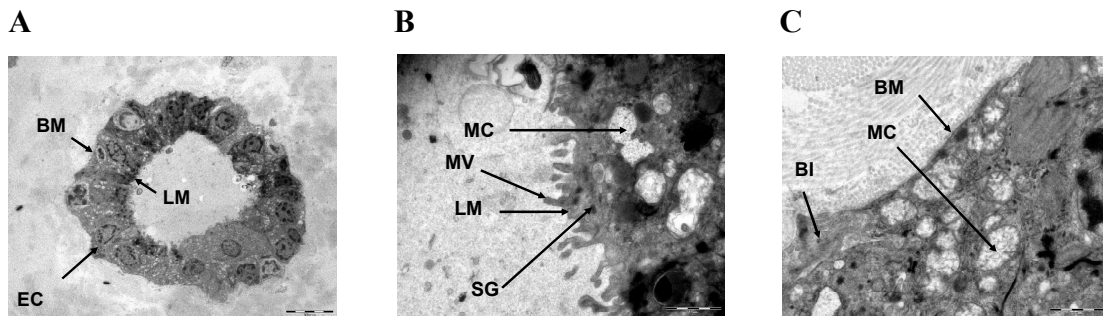


Figure 2. Electron micrographs of intact lacrimal ducts that had been maintained in culture for 24h. (A) Horizontal sections of isolated ducts. LM: luminal membrane, BM: basolateral membrane, EC: epithelial cell. **(B)** The luminal side of the lacrimal duct. MC: mitochondria, MV: microvilli, SG: secretory granule **(C)** The basolateral side of the lacrimal duct. BI: basolateral interdigitation. The bar represents 1 μm .

3.3.2. Resting pH_i of the lacrimal gland ductal epithelia

In the first series of experiments, we wanted to determine the resting pH_i of LGDC. Ducts were exposed to standard HEPES solution (pH:7.4), followed by an 8 min exposure to a high- K^+ -HEPES solution (pH: 7.28), and then to an 8 min exposure to a high- K^+ -HEPES solution (pH: 7.4). We used the classical linear model,^[60, 61] to determine the resting pH_i . The resting- pH_i level of 5 ducts (22 ROIs) was found to be 7.40 ± 0.01 . The resting pH_i of LGDC was virtually the same confirming that the experimental conditions can be kept constant for pH_i experiments (Fig. 3).

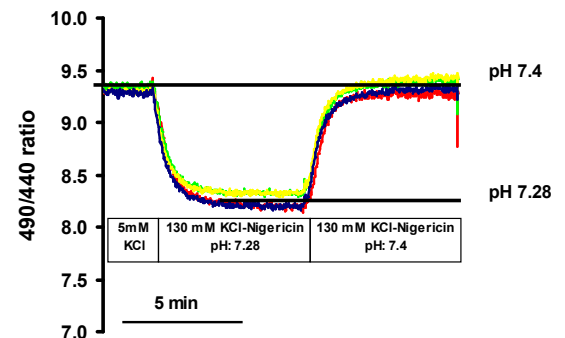


Figure 3. The resting pH_i of lacrimal ductal epithelial cells. Ducts were exposed to nigericin/high K^+ -HEPES solutions of pH 7.28 and 7.4. Due to the relatively short time course of the experiment, the resting pH_i was calculated from this 2-point calibration by using the classic linear model. In this particular experiment, the pH_i was 7.4. The resting pH_i of 5 ducts (22 ROIs) was 7.40 ± 0.01 .

3.3.3. Na⁺/H⁺ exchanger

In this series of experiments, we tested whether the isolated lacrimal glands are suitable for functional experiments. The Na⁺/H⁺ transport proteins that mediate the electroneutral exchange of Na⁺ and H⁺ ions were examined. Removal of Na⁺ from the standard Hepes solution caused a rapid and marked intracellular acidosis (0.20 ± 0.01 pH U/min, n=3 ducts / 15 ROIs) (Fig. 4A). Re-addition of Na⁺ to the solution resulted in a complete pH_i recovery. Since the solution did not contain HCO₃⁻, this finding confirms the presence of a Na⁺ dependent H⁺ efflux mechanism on the basolateral side of the LGDC. Removal of Na⁺ from the HCO₃⁻/CO₂ containing solution also caused a mark acidification (0.22 ± 0.04 pH U/min, n=3 ducts / 15 ROIs) (Fig. 4B).

3.3.4. Na⁺/HCO₃⁻ co-transporter

We also tested whether LGDC express a functionally active Na⁺ dependent HCO₃⁻ transporter on the basolateral membrane (Fig. 4B). Administration of basolateral HCO₃⁻/CO₂ rapidly and greatly decreased pH_i. This marked change in pH_i can be explained by the quick diffusion of CO₂ into the cytoplasm. A small pH_i recovery (0.04 ± 0.02 pH U/min, n=6 ducts / 30 ROIs) was found after the acidification suggesting the marginal role of HCO₃⁻ efflux into the lacrimal duct cells.

3.3.5. Cl⁻/HCO₃⁻ exchange activity

To test the activity of the Cl⁻/HCO₃⁻ exchange mechanisms we utilized the Cl⁻ removal technique in the presence and absence of HCO₃⁻ ions. In the absence of HCO₃⁻, Cl⁻ removal caused a small reversible alkalization in LGDC (Fig. 4C; 0.020 ± 0.002 pH U/min), suggesting the small availability of HCO₃⁻ ions in the cytoplasm. However, in standard HCO₃⁻/CO₂ solution a significantly higher alkalization was observed (Fig. 4D; 0.16 ± 0.02 pH U/min, respectively).

In addition, the anion exchange inhibitor H₂DIDS (250 μM) significantly inhibited ΔpH/Δt (Figs. 4E and F; 0.067 ± 0.015 pH U/min). These results confirm functionally active Cl⁻/HCO₃⁻ exchange mechanisms on the basolateral membrane of LGDC.

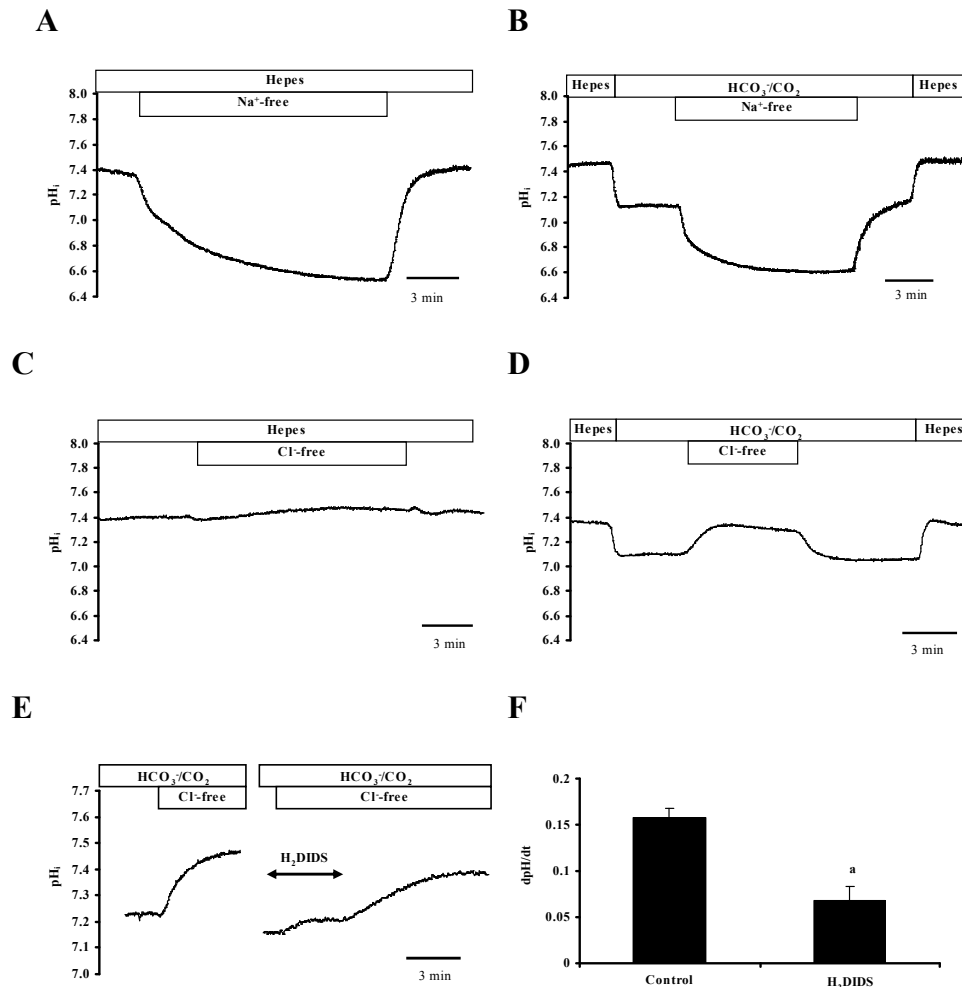


Figure 4. Effects of removal and readdition of extracellular Na^+ or Cl^- with and without HCO_3^-/CO_2 on pH_i in lacrimal ductal epithelial cells. (A) Removal of Na^+ resulted in a rapid reversible acidification of pH_i . (B) Standard HCO_3^-/CO_2 solution caused a rapid acidification of pH_i by the diffusion of CO_2 into the cells. Removal of Na^+ resulted in the same range of acidification as in Fig. 4A. (C) Removal of Cl^- from the HCO_3^- -free (Hepes) solution resulted in a small reversible alkalization of pH_i , while in a HCO_3^- containing solution (D) this pH_i change was enhanced. Traces are representative of 3 experiments for each protocol. (E). Removal of Cl^- from the standard HCO_3^-/CO_2 solution resulted in an alkalization of pH_i ; H_2DIDS (250 μM) strongly inhibited this alkalization, and this inhibitory effect of H_2DIDS was - at least partially - reversible. (F). Summary of the calculated initial rates of alkalization ($\Delta pH_i/\Delta t$) from Fig. 4E are shown. Means \pm SEM for 14 ROIs of 3 ducts are shown. a: $p < 0.05$ vs control.

3.3.6. pH_i recovery from alkali and acid load

An alternate method for characterizing the above mentioned transporters is the ammonium-pulse technique.^[63] Administration of 20 mM NH_4Cl initially increases pH_i due to the rapid entry of NH_3 into the cell. The recovery from alkali load may reflect the activity of the Cl^-/HCO_3^- exchanger.^[63] Removal of NH_4Cl causes the typical acidic undershoot of pH_i (Fig. 5A). The transporters (if present in LGDC) most likely involved in the recovery process from acidosis are the basolateral Na^+/HCO_3^- cotransporter, the Na^+/H^+ exchanger and the H^+ pump.

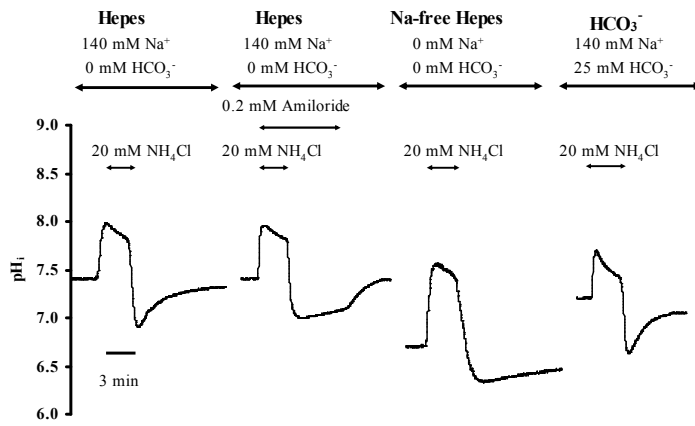
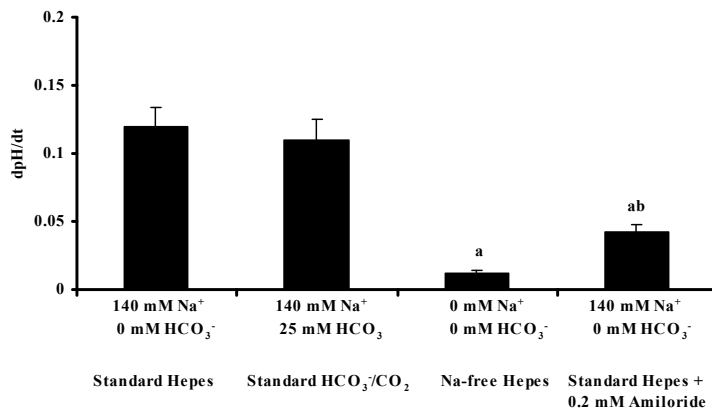
A**B**

Figure 5. Recovery of pHi after an acid load. (A). Duct cells were acid loaded by a 3 min exposure to 20 mM NH₄Cl, followed by its sudden withdrawal. The initial rates of pHi recovery from the acid load (over the first 30 s) were calculated in each experiment. All experiments were performed at 37°C using standard Hepes (with or without Na⁺) or HCO₃⁻/CO₂ solution, respectively. Each experiment was performed on a different duct. **(B).** Summary of the calculated initial rate of recovery ($\Delta\text{pH}/\Delta t$) from Fig. 5A are shown. The effects of different solutions (HCO₃⁻-free and/or Na⁺-free) and the NHE inhibitor, amiloride, are shown. Means \pm SEM for 30 ROIs of 6 ducts are shown. a: $p < 0.001$ vs. Standard Hepes. b: $p < 0.05$ vs. Na⁺-free Hepes.

The recovery ($\Delta\text{pH}/\Delta t$) from alkali load was significantly higher in the presence of HCO₃⁻ (0.049 ± 0.004 pH U/min and 0.08 ± 0.001 pH U/min, respectively) suggesting an active Cl⁻/HCO₃⁻ exchanger. The recovery from acid load was 0.12 ± 0.01 pH U/min in standard HCO₃⁻/CO₂ solution (containing Na⁺ and HCO₃⁻/CO₂). The absence of HCO₃⁻ did not significantly change the rate of recovery (0.11 ± 0.015 pH U/min). However, the removal of Na⁺ from the standard Hepes solution significantly decreased the recovery from acid load to 0.012 ± 0.002 pH U/min by switching off the Na⁺/H⁺ exchanger. The small remaining recovery from acid load may represent an active proton pump in LGDC. Finally, we tested the NHE inhibitor amiloride (0.2 mM). Amiloride administration greatly inhibited the Na⁺/H⁺ exchanger (0.04 ± 0.01 pH U/min) located on the basolateral membrane of LGDC. Furthermore, the removal of amiloride immediately turned on the Na⁺/H⁺ exchanger suggesting the reversible effect of amiloride.

3.3.7. Ca^{2+} signaling during parasympathomimetic stimulation

The parasympathetic neurotransmitters acetylcholine (ACh) and vasoactive intestinal peptide are potent stimuli of lacrimal gland secretion,^[67] and have been shown to act through the intracellular Ca^{2+} signaling pathway. The parasympathomimetic carbachol was administered to LGDC in 3 different doses (10, 100 and 1000 μM , Fig. 6). Carbachol dose dependently stimulated the intracellular Ca^{2+} signaling in LGDC (F/F_0 14 ± 0.1 , 20 ± 0.1 and $39 \pm 0.1\%$, respectively) suggesting the importance of this pathway in water and ion secretion. The parasympatholytic atropine (0.2 mM) completely blocked the stimulatory effect of carbachol (1 mM).

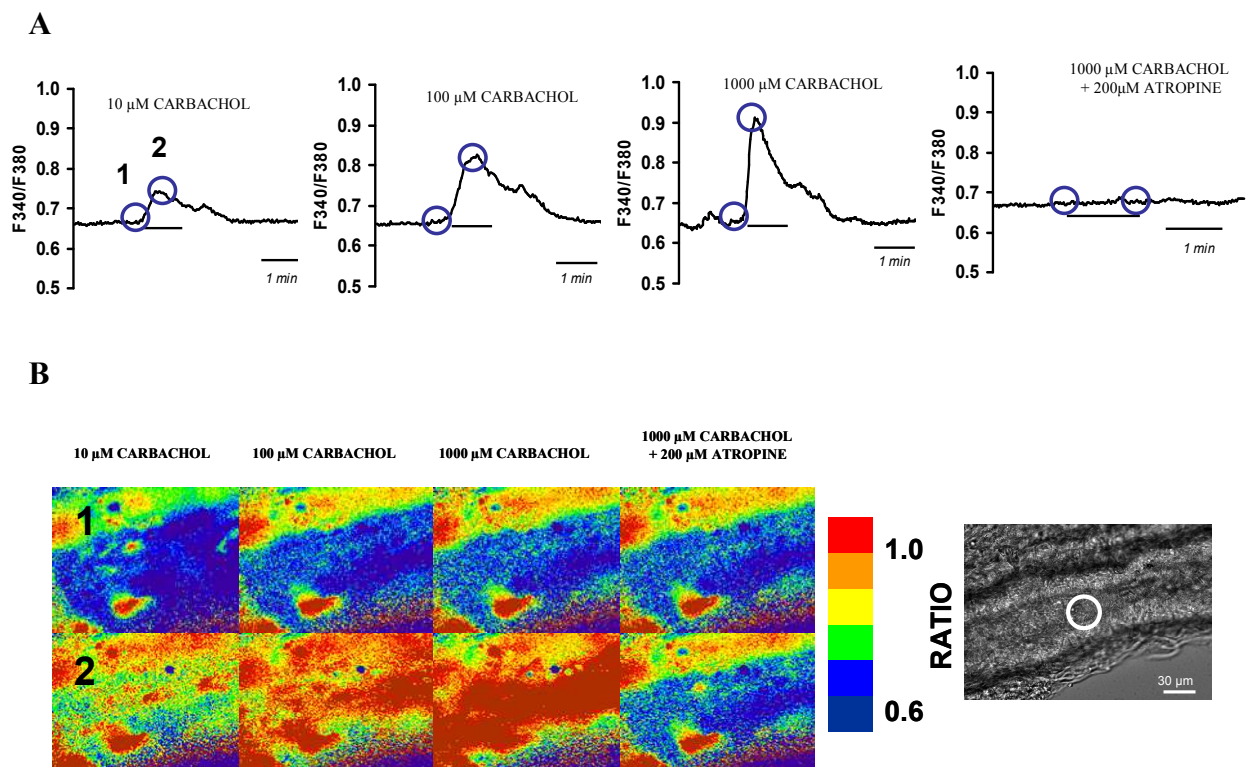


Figure 6. Effects of carbachol on intracellular Ca^{2+} concentration in lacrimal gland ductal epithelial cells. Cultured lacrimal ducts were attached to a coverslip as described in the methods. (A) 10, 100 and 1000 μM carbachol was administered to duct cells in standard HEPES solution. Carbachol dose dependently elevated $[\text{Ca}^{2+}]_i$. Each experiment was performed on the same duct using a 10 min wash-out period between the pulses. Representative curves are shown. Maximal $[\text{Ca}^{2+}]_i$ elevation was observed 2 ± 0.5 s after stimulation. Similar results were obtained when the experiments were performed on different ducts ($n=3$). (B) Shown are the typical patterns of $[\text{Ca}^{2+}]_i$ changes in an intact duct perfused with different concentrations of carbachol. Increase in $[\text{Ca}^{2+}]_i$ is denoted by a change from a “cold” color (blue) to a “warmer” color (yellow to red; see color scale on the top). Pictures 1-2 were taken at the times indicated by the circles in A. A representative duct is shown on the right. Data were taken from the ROI marked in the picture. The bar represents 30 μm .

3.3.8. The effects of carbachol on the Na^+/H^+ and anion exchangers

Administration of 1 mM carbachol significantly elevated the pH_i in standard Hepes solution (containing Na^+ and Cl^- , but no HCO_3^-) (Fig. 7A). However, this elevation was not observed in a Na^+ -free Hepes solution (Fig. 7B). Since HCO_3^- was absent, the alkalization in the Na^+ -containing solution must be due to a stimulated Na^+ dependent H^+ efflux mechanism via an NHE (Fig. 7A).

When the LGDCs were treated with 1 mM carbachol in standard $\text{HCO}_3^-/\text{CO}_2$ solution, a small pH_i elevation was observed (Fig. 7C). However, this brief alkalization (most likely caused by the stimulation of an NHE) of pH_i was followed by an acidification. Importantly, this acidification was absent in a Cl^- -free HCO_3^- solution suggesting that this decrease in pH_i is due to a Cl^- dependent HCO_3^- efflux mechanism via a $\text{Cl}^-/\text{HCO}_3^-$ exchanger (Fig. 7D). These data indicate that carbachol stimulates Na^+ and Cl^- influx into the cell through the basolateral membrane of LGDC. Importantly, the parasympatholytic atropine (0.2 mM) totally blocked the stimulatory effect of 1 mM carbachol (Fig. 7E).

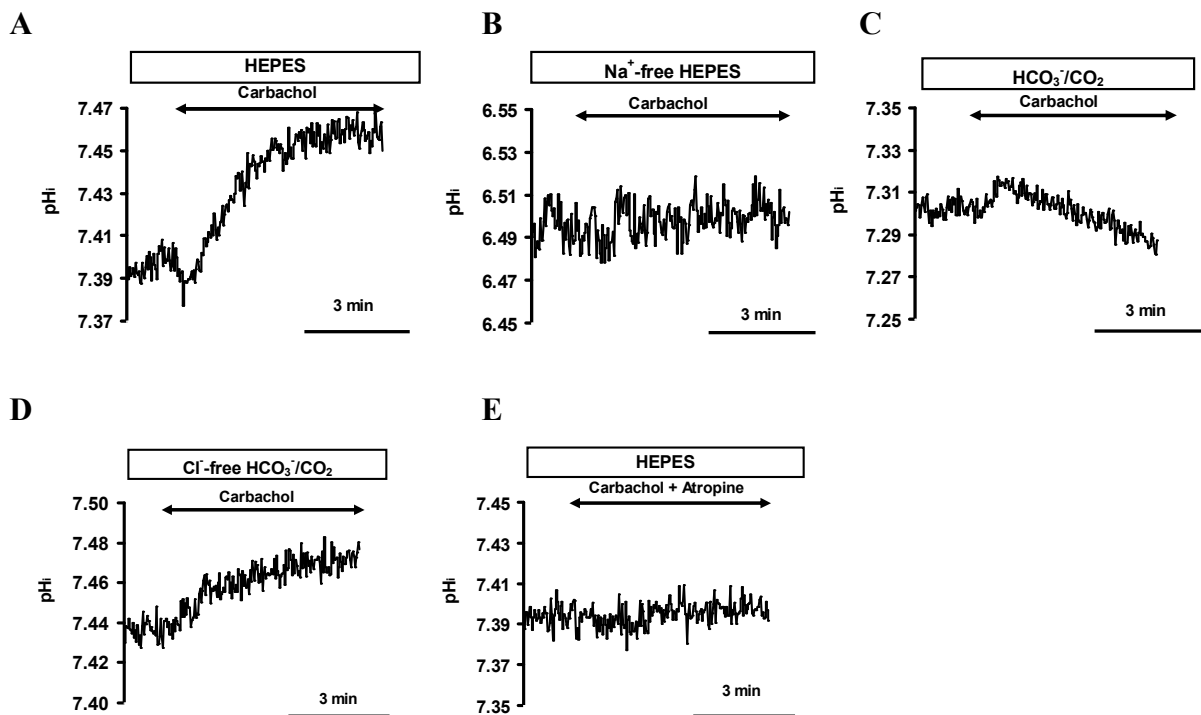
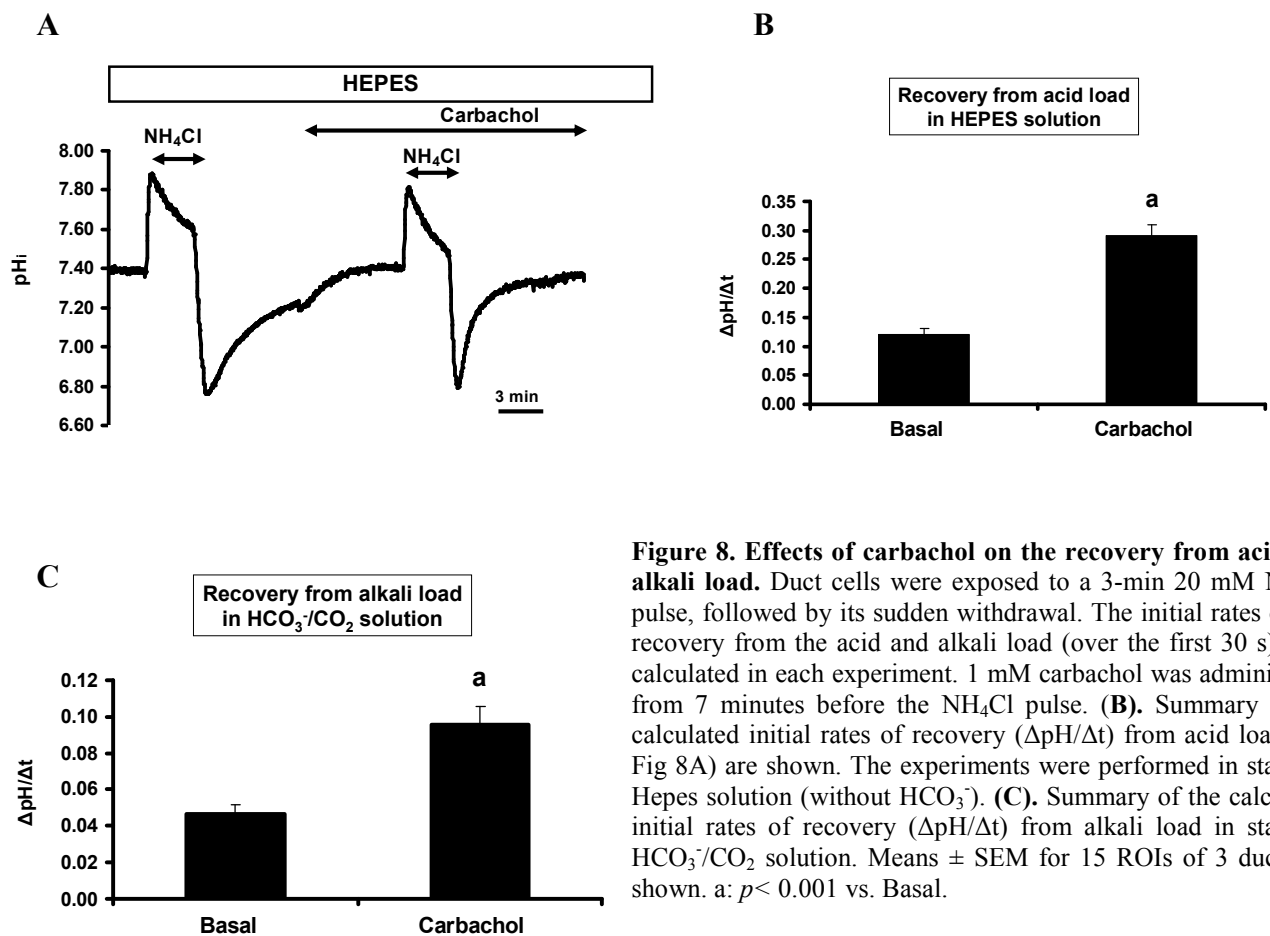


Figure 7. Effects of carbachol on pH_i . 1 mM carbachol was administered to duct cells in (A) standard Hepes solution (containing Na^+ and Cl^- , but no HCO_3^-), (B) Na^+ -free Hepes solution (containing Cl^- , but no Na^+ and HCO_3^-), (C) standard $\text{HCO}_3^-/\text{CO}_2$ solution (containing Na^+ , Cl^- and HCO_3^-) or (D) Cl^- -free $\text{HCO}_3^-/\text{CO}_2$ solution (containing Na^+ and HCO_3^- , but no Cl^-). (E) 1 mM carbachol and 200 μM atropine were administered to duct cells in standard Hepes solution. Please note that alkalization of pH_i was only observed in Na^+ containing solutions (A, C and D). Acidification of pH_i was observed only in a Cl^- and HCO_3^- -containing solution (C).

To confirm this hypothesis we analysed the recoveries from acid and alkali load using the ammonium pulse technique. Fig. 8 shows a representative trace of the experiments. We found that 1 mM carbachol significantly stimulated the NHE (recovery from acid load in a HCO_3^- free solution, Figs. 8A and B). No differences were observed in the recovery from alkali load in a HCO_3^- -free (Hepes) solution. However, when the experiments were performed in standard HCO_3^- solution, the AE (recovery from alkali load, Fig. 8C) was stimulated by 1 mM carbachol. As we found earlier, atropine (0.2 mM) totally blocked the stimulatory effect of carbachol on the NHE and AE (data not shown).



3.3. Differential effect of bile acids on pancreatic ductal cells

3.3.1. Effect of basolateral exposure to bile acids on duct cell pH_i

Figure 9A-D shows the effect of basolateral administration of the non-conjugated CDC and the conjugated GCDC on the duct cell pH_i in perfused pancreatic ducts.

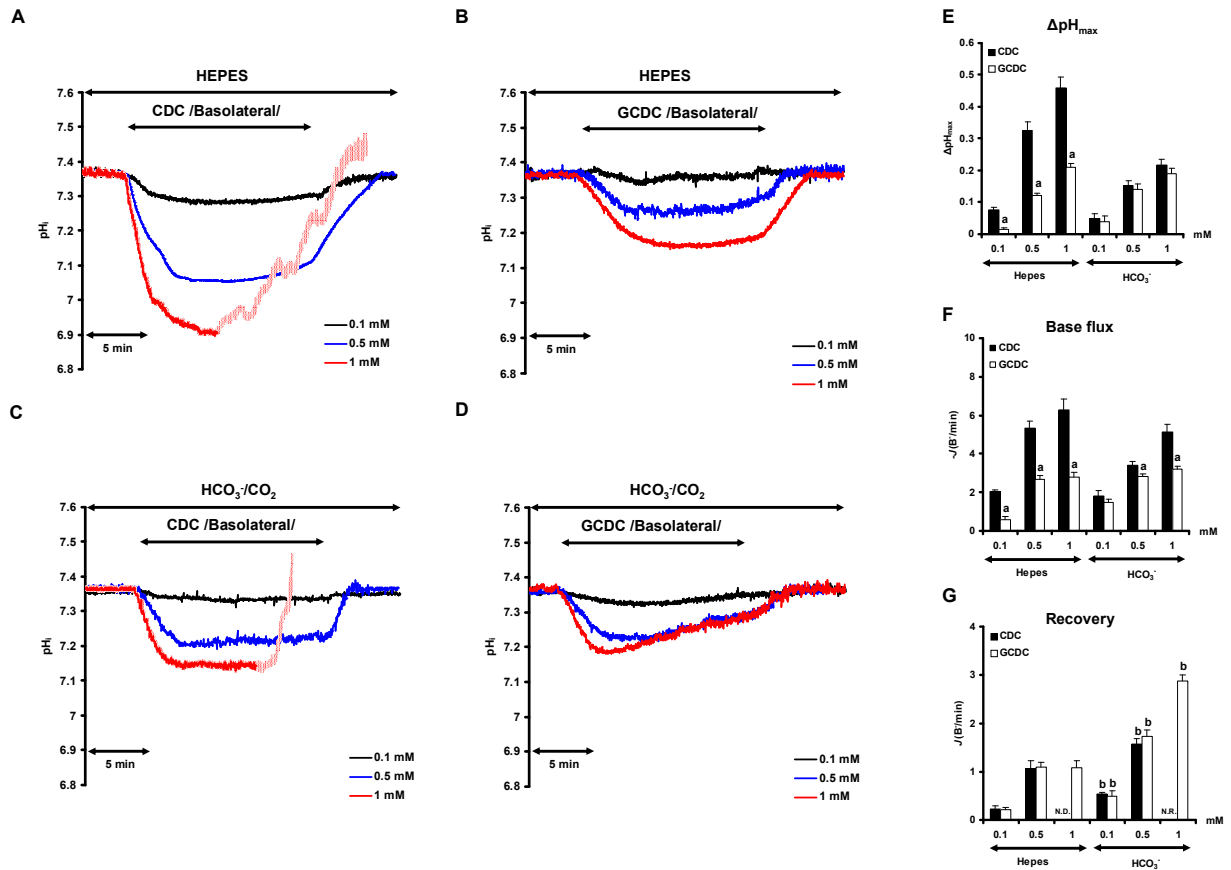


Figure 9. Effect of basolateral administration of bile acids on intracellular pH_i and base flux of pancreatic duct epithelial cells (PPDC). Panels A and B show representative pH_i traces demonstrating the effect of chenodeoxycholate (CDC; 0.1, 0.5, 1 mM) and glycochenodeoxycholate (GCDC; 0.1, 0.5, 1 mM) administered from the basolateral membrane in $\text{HCO}_3^-/\text{CO}_2$ and in standard HEPES-buffered solution (C and D). Summary data of the maximal pH_i changes ($\Delta\text{pH}_{\text{max}}$), are shown in panel E and the mean base (bile acid) flux ($-J(\text{B}')$), in panel F. Panel G shows the recoveries ($J(\text{B}')$) during the addition of bile acids. Means \pm SEM are from 36 regions of interests (ROIs) of 8 ducts. a: $p < 0.001$ vs. CDC; b: $p < 0.001$ vs. HEPES. N.D.: not detectable, N.R.: not recordable (due to dye leakage).

Typically, the response was an initial rapid, dose-dependent, fall in pH_i which then recovered to a variable degree during continued exposure to the bile acids. Note that the effect of the bile acids on pH_i was greatest in standard HEPES-buffered as compared to HCO_3^- -buffered solutions (Figs. 9A-D). Also, when 1mM CDC was administered in standard HEPES solution, the fluorescence intensities at 440 and 490nm rapidly decreased after 6 ± 1 min ($n = 6$ ducts/35ROIs), causing an elevation of the 490/440 ratio (Fig. 9A). This rapid decrease of the fluorescence intensities must be due to loss of BCECF from the cells. The presence of $\text{HCO}_3^-/\text{CO}_2$ delayed this event somewhat to 8 ± 1 min ($n = 6$ ducts/38ROIs) (Fig. 9C). However, no dye leakage occurred with the same concentration of the conjugated GCDC (Figs. 9B and D).

The maximal pH_i change ($\Delta\text{pH}_{\text{max}}$) and the base flux ($J(\text{B}^-)$) following exposure to the bile acids were calculated for each experiment and the summary data are shown in figures 9E and F. In standard HEPES-buffered solutions the unconjugated CDC had a much larger effect on $\Delta\text{pH}_{\text{max}}$ and $J(\text{B}^-)$ than the conjugated GCDC, most likely explained by slower permeation of the charged GCDC into the duct cells. In contrast, in $\text{HCO}_3^-/\text{CO}_2$ containing solutions the bile salts induced much smaller changes in $\Delta\text{pH}_{\text{max}}$ and $J(\text{B}^-)$ (Figs. 9E and F). This was particularly obvious for the unconjugated CDC and is consistent with the increased buffering capacity of the duct cells in the presence of $\text{HCO}_3^-/\text{CO}_2$.^[58]

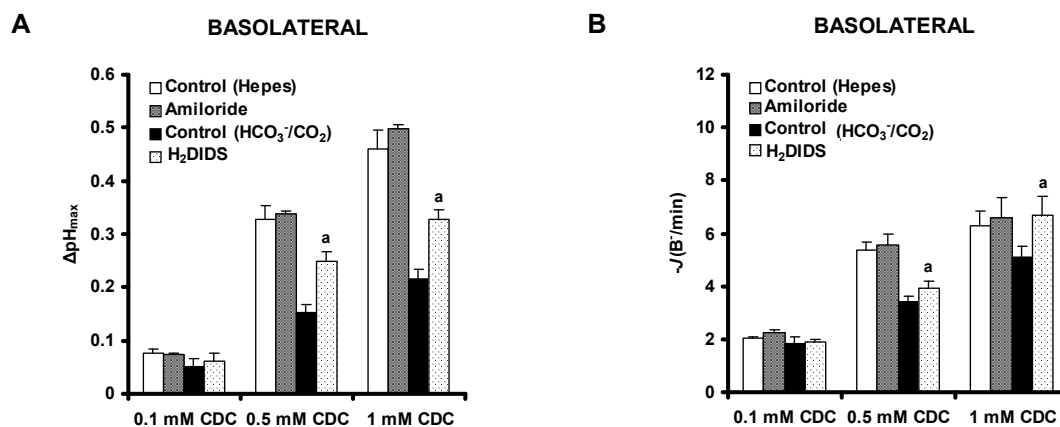


Figure 10. The effects of NBC and NHE activity on the CDC-induced acidification. Panels A and B show the effect of 0.5 mM H_2DIDS in $\text{HCO}_3^-/\text{CO}_2$ buffered solution or 0.2 mM amiloride in standard HEPES-buffered solution on the bile induced base flux ($-J(\text{B}^-)$) and $\Delta\text{pH}_{\text{max}}$ from the basolateral membrane. We found that amiloride did not have any effect on the initial phase of bile acid induced acidification or on the $\Delta\text{pH}_{\text{max}}$. However, in the presence of H_2DIDS the rate of acidification and the CDC-induced pH_i change was significantly higher. Means \pm SEM are from 23 ROIs of 4 ducts. a: $p < 0.001$ vs the respective control.

Amiloride (0.2 mM) had no effect on the $\Delta\text{pH}_{\text{max}}$ and $J(\text{B}^-)$ caused by basolateral exposure to the unconjugated CDC in a standard Hepes-buffered solution, suggesting that Na^+/H^+ exchange is not activated during the acidification process (Figs. 10A and B). However, basolateral administration of 0.5 mM H_2DIDS significantly increased both the $\Delta\text{pH}_{\text{max}}$ and the $J(\text{B}^-)$ in response to CDC (Figs. 10A and B). This result suggests that the basolateral NBC normally acts to attenuate the fall in pH_i caused by CDC, presumably by transporting HCO_3^- ions into the duct cells.

3.3.2. Effect of luminal exposure to bile acids on duct cell pH_i

Figure 11A-F shows the effect of luminal administration of the bile acids on duct cell pH_i and $J(\text{B}^-)$ in perfused pancreatic ducts.

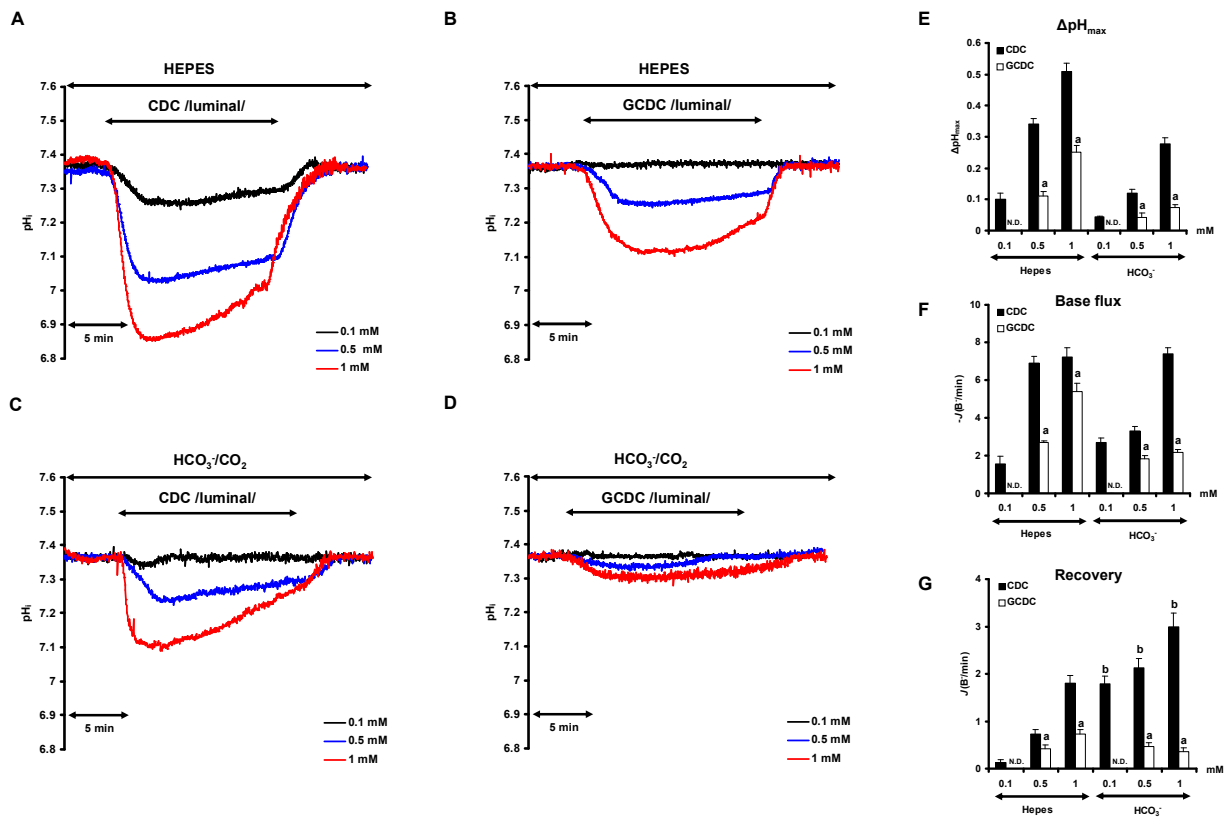


Figure 11. Effect of luminal administration of bile acids on intracellular pH (pH_i) and base flux of pancreatic duct epithelial cells. Panels A and B show representative pH_i traces demonstrating the effect of chenodeoxycholate (CDC; 0.1, 0.5, 1 mM) and glycochenodeoxycholate (GCDC; 0.1, 0.5, 1 mM) administered from the luminal membrane in $\text{HCO}_3^-/\text{CO}_2$ and in standard Hepes-buffered solution (C and D). Summary data of the maximal pH_i changes ($\Delta\text{pH}_{\text{max}}$) are shown in panel E and the mean base (bile acid) flux ($-J(\text{B}^-)$), in panel F. Panel G shows the recoveries ($J(\text{B}^-)$) during the addition of bile acids. Means \pm SEM are from 26 regions of interests (ROIs) of 5 ducts. a: $p < 0.001$ vs. CDC; b: $p < 0.001$ vs. Hepes. N.D.: not detectable.

As with basolateral exposure, there was: (i) a rapid fall in pH_i followed by a variable degree of pH_i recovery during continued exposure to the bile acid, (ii) the unconjugated CDC caused a much larger $\Delta\text{pH}_{\text{max}}$ and $J(\text{B}^-)$ than the conjugated GCDC, and (iii) luminal bile acids had a larger effect on pH_i when tested in a standard Hepes solution as compared to a $\text{HCO}_3^-/\text{CO}_2$ solution (Figs. 11A-F). However, note that luminal exposure to 1 mM CDC never caused the rapid dye loss that occurred following basolateral addition of the bile acid.

3.3.3. Recovery of duct cell pH_i during continued exposure to bile acids

The experimental traces in Figures 9 and 11 indicate that some degree of pH_i recovery occurred during continuous exposure of the pancreatic duct epithelial cells (PPDC) to bile acids; except with 1 mM CDC administered from the basolateral side which damages the cells and causes dye leakage (Fig. 9). Initially, we calculated the $J(\text{B}^-)$ values during pH_i recovery with and without $\text{HCO}_3^-/\text{CO}_2$. A partial recovery of pH_i during continuous exposure to the bile salts (except 1 mM basolateral CDC) occurred in both Hepes and $\text{HCO}_3^-/\text{CO}_2$ solutions (Figs. 9A-D and Figs. 11 A-D). However, the calculated $J(\text{B}^-)$ values during pH_i recovery following basolateral administration of CDC and GCDC were 1.5- to 2.5-fold higher in the presence of $\text{HCO}_3^-/\text{CO}_2$ (Fig. 9G). Similarly, $\text{HCO}_3^-/\text{CO}_2$ enhanced the $J(\text{B}^-)$ during pH_i recovery following luminal exposure to CDC (Fig. 11G). However, no such effect was seen with luminal GCDC (Fig. 11G), presumably because luminal GCDC caused only small changes in duct cell pH_i under these conditions (Fig. 11D).

We sought to establish which acid/base transporters are involved in the pH_i recovery process; the most likely candidates being the basolateral NBC and the NHE.^[68] Fig. 12A shows that amiloride (0.2 mM) strongly inhibited the $J(\text{B}^-)$ during pH_i recovery following exposure to basolateral CDC (0.1 and 0.5 mM) in standard Hepes solution, suggesting a major role for the NHE in pH_i recovery in the absence of HCO_3^- ions. In a more physiological $\text{HCO}_3^-/\text{CO}_2$ solution, amiloride was a somewhat less effective inhibitor (Fig. 12B). This suggests an involvement of the NBC in pH_i recovery when HCO_3^- is present and is consistent with the enhancing effect of $\text{HCO}_3^-/\text{CO}_2$ on $J(\text{B}^-)$ during pH_i recovery (Figs. 9G and 11G). Taken together, these data suggest that, when it occurs, pH_i recovery during exposure to bile acids is mediated both by the NHE and the NBC.

When a high dose of CDC (1 mM) was administered to the basolateral membrane in standard Hepes solution, PPDC started to lose dye and so pH_i recovery could not be studied (Fig. 9A). Leakage of dye was delayed in a $\text{HCO}_3^-/\text{CO}_2$ solution, however, no pH_i recovery

was observed before the cell membrane became permeable suggesting that the NBC and NHE were totally inhibited under these conditions (Fig. 9C).

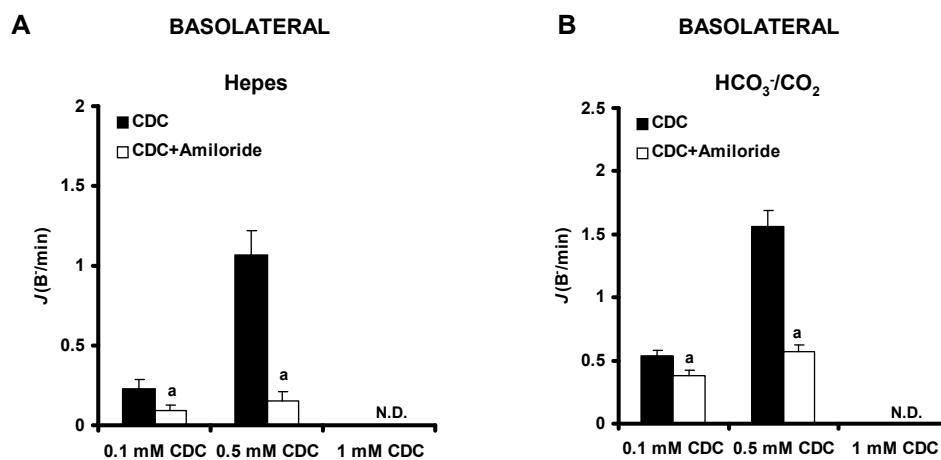


Figure 12. Amiloride inhibits the recovery of pH_i during chenodeoxycholate administration. Panels A and B show the effect of 0.2 mM amiloride on the recovery of pH_i during CDC administration (0.1, 0.5 and 1 mM) in the absence or presence of $\text{HCO}_3^-/\text{CO}_2$. We found that amiloride inhibited the recovery during CDC administration. However, this inhibitory effect was significantly lower in the presence of $\text{HCO}_3^-/\text{CO}_2$, which indicates that NBC is involved in the recovery process. Means \pm SEM are from 27 ROIs of 5 ducts. a: $p < 0.001$ vs the respective control. N.D.: not detectable.

3.3.4. Effect of bile acids on HCO_3^- secretion

To investigate the effects of bile acids on HCO_3^- secretion, we analysed the recovery of pH_i from an alkali load induced by exposure to NH_4Cl in a $\text{HCO}_3^-/\text{CO}_2$ containing solution (for original traces see Fig. 13). We have previously shown that the $J(\text{B})$ calculated from the rate of pH_i recovery under these conditions reflects the rate of HCO_3^- efflux (i.e. secretion) on luminal $\text{Cl}^-/\text{HCO}_3^-$ exchangers.^[68] Basolateral administration of a low dose (0.1 mM) of the unconjugated CDC had no effect on $J(\text{B})$; however, a higher dose of CDC (1 mM) strongly inhibited HCO_3^- secretion (Fig. 14A). Interestingly, luminal administration of 0.1 mM CDC had a stimulatory effect on HCO_3^- secretion (Fig. 14B), whereas the higher dose (1 mM) was inhibitory (Fig. 14B). The basal rate of HCO_3^- secretion and the stimulatory effect of luminal 0.1 mM CDC were unaffected by bumetanide or bromsulphophthalein (Fig. 14C), suggesting that neither the $\text{Na}^+/\text{K}^+/\text{2Cl}^-$ cotransporter nor bile acid/ HCO_3^- exchange on the organic anion transporter protein (OATP) were involved in pH_i recovery (Fig. 14C). In contrast to the effects of CDC, neither basolateral nor luminal application of the conjugated GCDC (0.1 and 1 mM) had any effect on pH_i recovery from an alkali load (Figs. 14A and B).

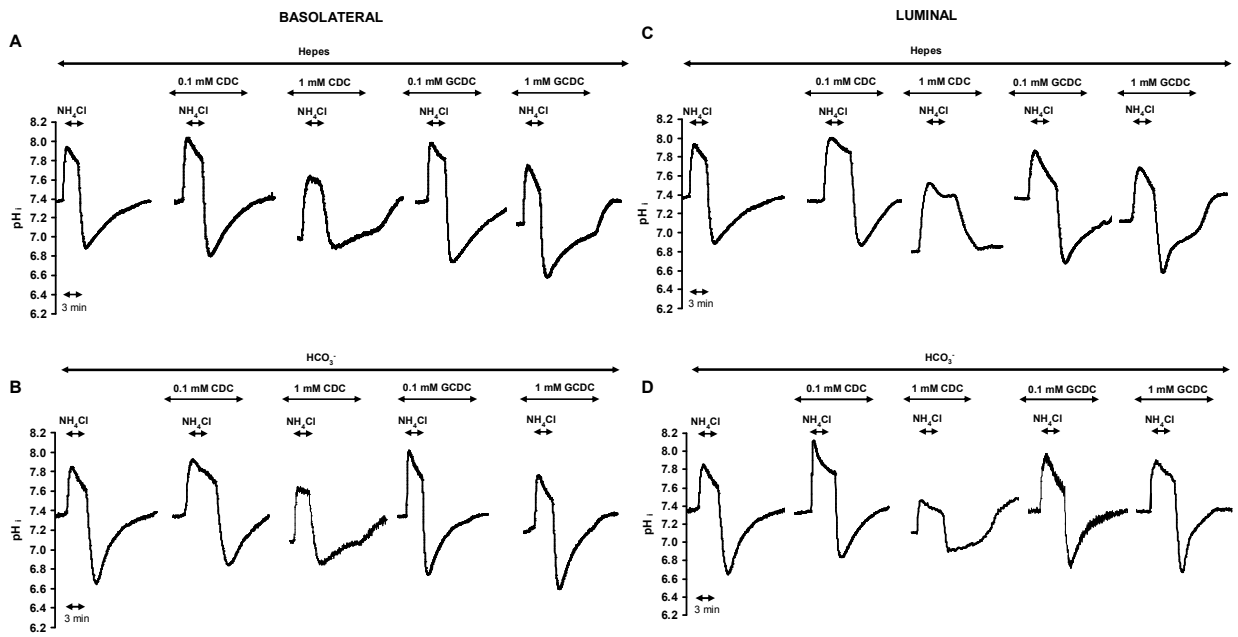


Figure 13. Effect of bile acids on the rate of pH_i recovery from an acid load. Panels A-D show the effect of bile acids (0.1 mM and 1 mM) administered from the basolateral membrane (A and B) or from the luminal membrane (C and D) on pH_i recovery from an acid load (20 mM NH₄Cl) in the absence (A and C) or presence (B and D) of HCO₃⁻/CO₂. GCDC had no significant effect on the rate of pH_i recovery at either concentration, indicating that GCDC does not have a direct effect on the activity of NHE and NBC. In contrast, 1 mM CDC strongly inhibited the recovery from both the luminal and basolateral membranes in standard Hepes and HCO₃⁻/CO₂ (blank bars) buffered solutions (E and F). Means ± SEM are from 25 ROIs of 5 duct.

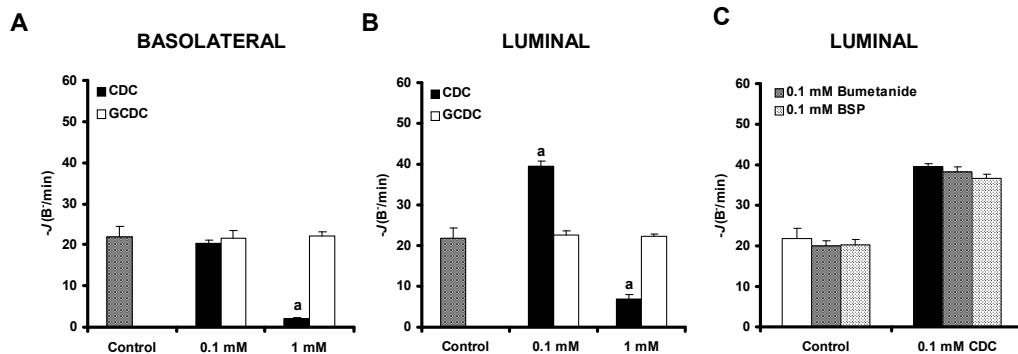


Figure 14. Effect of bile acids on the rate of pH_i recovery from an alkali load. Panel A shows the effect of basolaterally administered CDC (black bars) or GCDC (white bars) (0.1 mM and 1 mM) on the rate of pH_i recovery from an alkali load (20 mM NH₄Cl in HCO₃⁻/CO₂-buffered solution). A low concentration (0.1 mM) of CDC had no effect with respect to control, while 1 mM CDC strongly inhibited HCO₃⁻ efflux. In contrast 0.1 mM CDC administered from the luminal membrane (B) caused a significant increase in HCO₃⁻ secretion, whereas the high concentration (1 mM) blocked it. Panel C shows that the stimulatory effect of low dose CDC was not inhibited by bumetanide (0.1 mM) and bromsulphotalein (0.1 mM), inhibitors of the Na⁺K⁺2Cl⁻ cotransporter, and the Oatp transporter, respectively. The initial rate of pH_i recovery was calculated in each experiment. Means ± SEM are from 25 ROIs of 5 ducts. a: p < 0.001 vs control.

We used luminal H₂DIDS to investigate whether the stimulatory effect of luminal 0.1 mM CDC on HCO₃⁻ secretion was due to activation of Cl⁻/HCO₃⁻ exchangers. We found that H₂DIDS inhibited the basal rate of HCO₃⁻ secretion by about 65% and completely blocked the stimulatory effect of 0.1 mM luminal CDC, suggesting that the stimulatory effect must involve activation of luminal Cl⁻/HCO₃⁻ exchangers (Fig. 15A). We confirmed these results using another method of measuring HCO₃⁻ secretion – the inhibitor stop technique.^[63, 64] Again we found that luminal H₂DIDS totally blocked the stimulatory effect of low doses of CDC on HCO₃⁻ secretion (Fig. 15B).

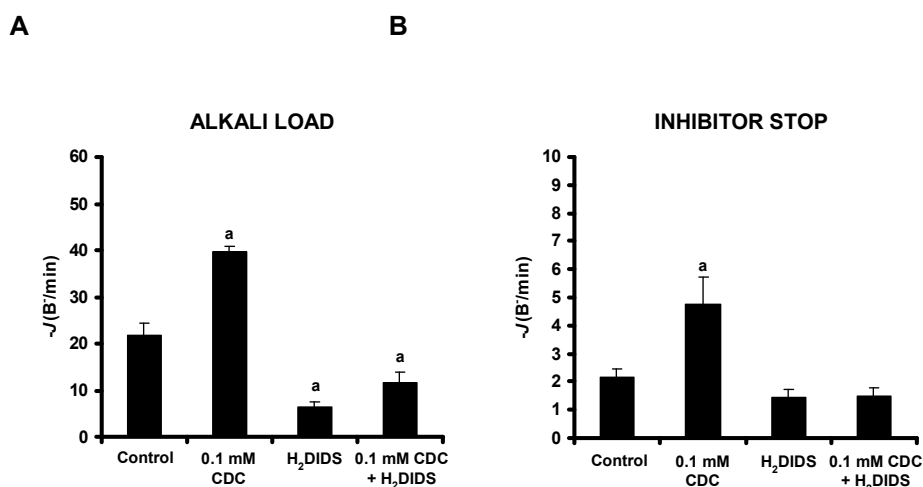


Figure 15. The luminal Cl⁻/HCO₃⁻ exchanger is involved in the stimulatory effect of low doses of non-conjugated bile acids administered from the luminal side. Panel A shows the effect of CDC (0.1 mM) on the rate of pH_i recovery from an alkali load (20 mM NH₄Cl) in the presence and absence of 0.5 mM luminal H₂DIDS. Panel B shows the inhibitor stop method for determining HCO₃⁻ secretion. PPDC were exposed to 0.2 mM amiloride and 0.5 mM H₂DIDS which caused a marked decrease in pH_i due to the inhibition of NHE and NBC. The experiments were performed in the presence or absence of 0.5 mM luminal H₂DIDS. In the test experiments the bile acid was administered into the lumen from 5 minutes before exposure to 0.5 mM H₂DIDS and 0.2 mM amiloride, or 20 mM NH₄Cl. The initial rate of acidification was calculated in each experiment. Means ± SEM are from 25 ROIs of 5 ducts. a: p<0.001 vs control.

Finally, we directly measured the effects of CDC on the activity of luminal Cl⁻/HCO₃⁻ exchangers using the Cl⁻ removal technique. Figure 16A shows that CDC (0.1 mM) strongly stimulated pH_i alkalinization after removal of luminal Cl⁻. The calculated $J(B^-)$ values indicate that base flux through the exchangers was increased about 8-fold under these conditions (Fig. 16B). Note that the rate of pH_i alkalinization and $J(B^-)$ on luminal Cl⁻ withdrawal were also slightly elevated when 1 mM CDC was used (which inhibits HCO₃⁻ secretion) (Figs. 16A and B). However, this apparent stimulation of anion exchange activity is most probably explained by the ongoing recovery of the pH_i that occurs during luminal administration of 1 mM CDC (see Fig. 11C).

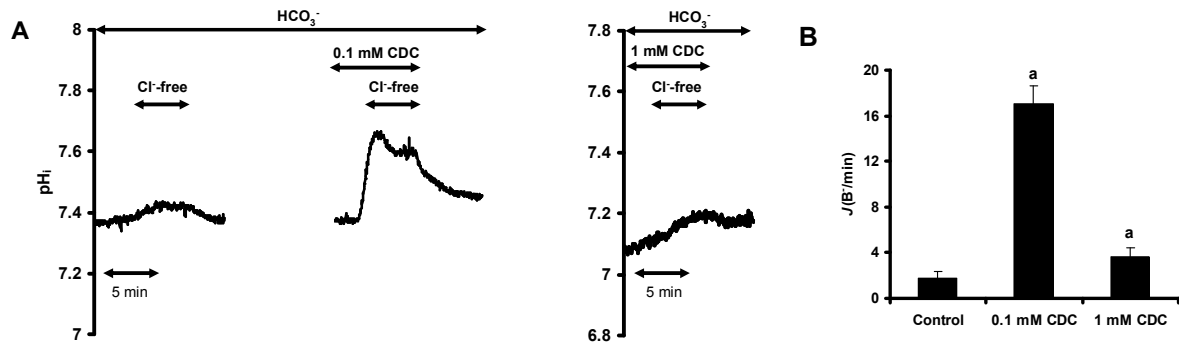


Figure 16. Effect of chenodeoxycholate on pH_i changes after Cl⁻ removal. Panel A shows representative traces demonstrating the effect of luminal CDC (0.1 and 1 mM) on pH_i changes after luminal Cl⁻ removal. 0.1 mM CDC induced a considerable increase both in the pH_i and in the maximal rate of alkalization. 1 mM CDC caused a slight increase in pH_i probably as a result of the activation of NBC and NHE. Panel B shows the summary data of the mean base (bile acid) flux ($J(B^-)$). Means \pm SEM are from 32 ROIs of 6 ducts. a: $p < 0.001$ vs control.

3.3.5. Relationship between the inhibitory and stimulatory effects of chenodeoxycholate on HCO₃⁻ secretion and chenodeoxycholate-induced changes in [Ca²⁺]_i

We have clearly shown that luminal administration of low doses of CDC (i) stimulate HCO₃⁻ secretion through the luminal membrane and (ii) induce an IP₃-mediated [Ca²⁺]_i elevation. Therefore, we investigated whether preventing the elevation of [Ca²⁺]_i using the intracellular Ca²⁺-chelator BAPTA-AM, had any effects on HCO₃⁻ secretion stimulated by luminal administration of low doses of CDC, using the alkali load method. We found that 40 μ M BAPTA-AM inhibited basal HCO₃⁻ secretion by about 25 % and totally blocked the stimulatory effect of low doses of CDC on HCO₃⁻ secretion (Fig. 17A). Finally, we examined whether Ca²⁺ signaling evoked by a high dose of CDC modulates the inhibitory effect of this non-conjugated bile acid. In contrast to the stimulatory effect of low doses of CDC, the Ca²⁺-chelator BAPTA-AM had no effect on the inhibitory effect of high doses of CDC (Fig. 17B).

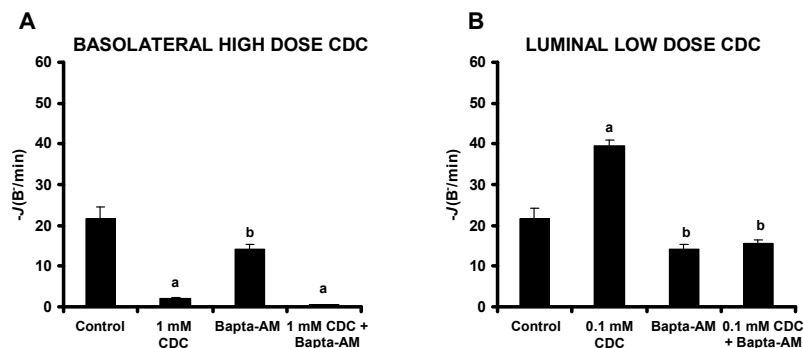


Figure 17. Elevation of intracellular Ca²⁺ concentration is responsible for the stimulatory effect of low doses of chenodeoxycholate on pancreatic HCO₃⁻ secretion. Panel A shows the effect of 40 μ M BAPTA-AM pretreatment (30 minutes before the experiments) on the stimulatory effect of 0.1 mM CDC from the luminal membrane. (B) The effect of BAPTA-AM (40 μ M) pretreatment on the inhibitory effect of 1 mM CDC from the basolateral membrane. Means \pm SEM are from 25 ROIs of 5 ducts. a: $p < 0.001$ vs. control, b: $p < 0.05$ vs. control.

3.4. The influence of hyperlipidemia on pancreatic HSP72 and IκB-α expression in acute necrotizing pancreatitis

We assessed if hyperlipidemia induced by cholesterol enriched diet affected the production of HSP72 in the pancreas in response to necrotizing pancreatitis. In the pancreas of the control rats, the basal level of HSP72 was very low, but the cholesterol-enriched diet significantly increased its expression. Arg-induced necrotizing pancreatitis resulted in further significant increases in pancreatic HSP72 content both in the animals on a normal diet and also in those on a high cholesterol diet as compared with the controls (Fig. 18A and B). Pancreatic IκB-α levels were not altered by cholesterol treatment vs the control. However, Arg administration significantly decreased IκB-α expression and this was further reduced in pancreatic rats on a cholesterol diet (Fig. 19).

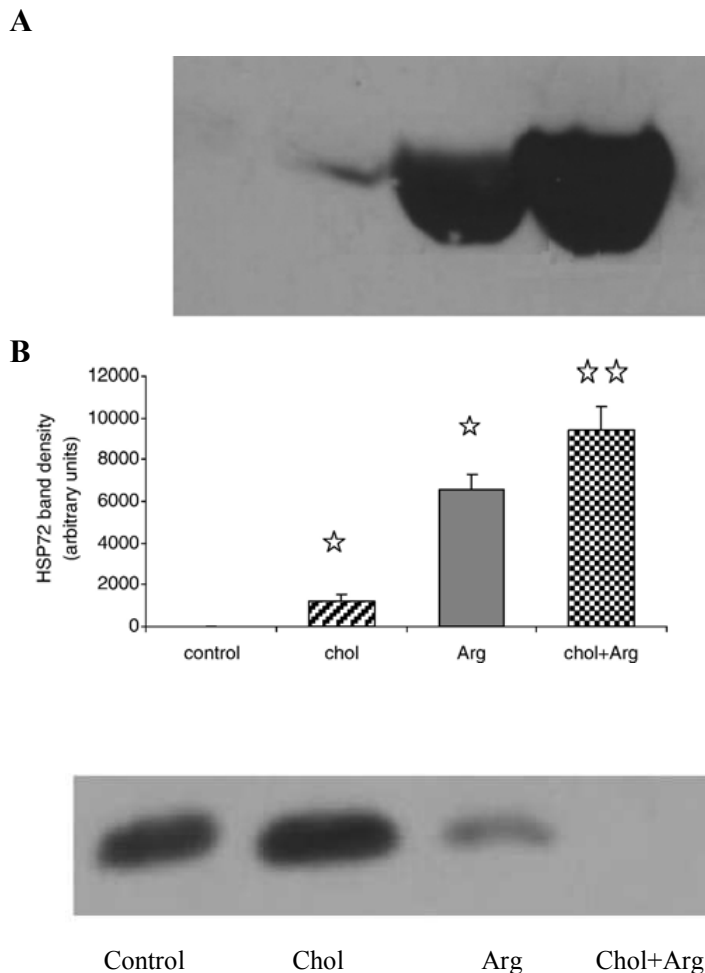


Figure 18. Pancreatic HSP72 expression is increased in hyperlipidemic rats.

A. Representative Western immunoblot analysis of protein lysates (40 μg/lane) from the pancreata of rats. **B.** The bar diagram shows the densities of the Western blot bands in the control, cholesterol-fed (chol) groups, and in normal and hyperlipidemic rats with necrotizing pancreatitis (Arg and chol + Arg). The densities of the Western blot bands were quantified by using the ImageJ software. Results are means ± S.E.M. (n=7). ☆: significant difference (P<0.05) vs. control group. ☆☆: significant difference (P<0.05) vs. chol group.

Figure 19. Pancreatic IκB-α levels.

Pancreatic cytosolic protein fractions were analyzed by Western blot analysis (40 μg/lane), using a specific IκB-α antibody. Rats were treated in the same manner as described in the legend to Fig. 18.

4. DISCUSSION

In the first part of this thesis we described the secretory mechanisms of the gastric and lacrimal glands under normal conditions.

The secretion of the exocrine gastric gland is a complex process regulated by neural and hormonal mechanisms. One of the most important factors in the hormonal regulation is gastrin. It has been clear for some years that Gas-KO mice have substantially reduced gastric acid secretion and an inability to respond to the major gastric acid secretagogues but the relevant cellular mechanisms are largely unknown.^[13, 14] The present studies made extensive use of cultured gastric glands. This preparation was selected because glands contain all the relevant cell types, and particularly histamine-secreting ECL cells, as well as parietal cells thereby facilitating studies of paracrine mechanisms. Using a protocol in which pH_i was employed to reflect H^+/K^+ ATPase activity we showed that parietal cells from Gas-KO mice were refractory to the action of gastrin, but exposure to G17 for 24 hr restored responses to those seen in glands from wild-type mice. Crucially, the effect of near-physiological concentrations of gastrin in this system was mediated by histamine. However, the priming effect of gastrin was not blocked by the H-2 receptor antagonist, ranitidine. The present data are therefore compatible with the idea that while histamine released from ECL cells is a mediator of the acute, secretagogue effect of gastrin, but it does not mediate the effect of gastrin on parietal cell priming, and instead raises the possibility that gastrin acts directly on CCK-2 receptors on parietal cells to stimulate parietal cell maturation.

Lacrimal gland secretion consists of two fractions derived from the acinar and ductal cells. The regulation of ion and water secretion has been well investigated in intact glands,^[67] however, no available method has been described to study the role of LGDC in the process of lacrimal fluid secretion. The precorneal tear secreted by the lacrimal gland contains Na^+ , Cl^- and K^+ in high concentration. This lacrimal gland fluid contains (mmol/L): $42 \pm 4 K^+$, $107 \pm 4 Na^+$, $126 \pm 5 Cl^-$ in rabbit^[69]; $46 \pm 3 K^+$, $135 \pm 5 Na^+$, $123 \pm 1 Cl^-$ in rat^[70] and $38 \pm 5 K^+$, $144 \pm 5 Na^+$, $149 \pm 16 Cl^-$ in mouse^[71]. The ductal epithelia, at least in part, must be involved in this hypertonic fluid secretion. In the present study we developed an isolation technique which is suitable to investigate the ion transporters of LGDC and the regulation of fluid secretion. The micro-dissection technique is very similar to what we used for the pancreas.^[60, 63] In order to show the viability of isolated and cultured interlobular lacrimal ducts, we characterized the most common acid/base transporters.

Our results showed the functional presence of a Na^+ -dependent but HCO_3^- -independent H^+ efflux mechanism (most probably through NHEs) on LGDC. Amiloride partially inhibited this Na^+/H^+ exchange mechanism. However, we must note that this K^+ sparing diuretic can also inhibit electrogenic Na^+ channels^[72] and the $\text{Na}^+/\text{Ca}^{2+}$ exchanger.^[73] Since NHE1 and 2 are the most sensitive to amiloride inhibition while NHE3 and 4 are amiloride resistant,^[74] our results indicate that approximately 66% of the functionally active NHEs are NHE1 and 2 isophorms. Many epithelial cells express proton pumps^[26] and NBC^[75] which, beside other physiological roles, can protect the epithelial cells from acidosis. We demonstrated that NBC ion transporters – if present - have only a marginal role in the pH_i regulation of LGDC. Following a CO_2 -induced acidosis, only a small amount of HCO_3^- entry was detected (see Fig. 5B). Furthermore, no difference was found in the regeneration after acid load caused by an ammonium pulse between the presence and absence of HCO_3^- . Removal of Na^+ decreased this recovery by 93 % in standard Hepes solution suggesting a functionally very active Na^+ dependent H^+ efflux mechanism. We also detected a functionally active Cl^- dependent HCO_3^- efflux mechanism in LGDC. When HCO_3^- was absent from the solution, Cl^- removal only caused a small pH_i change, suggesting a reduced HCO_3^- concentration inside the cell. However, when HCO_3^- was present in the solution, Cl^- removal caused a marked pH_i elevation. We found that the classic and defining inhibitor of SLC4 family AE1-AE4,^[76, 77] H_2DIDS , strongly inhibited the Cl^- dependent HCO_3^- efflux mechanism. AE1 has been identified in rat lacrimal ducts.^[21] However, no other AEs have been confirmed in lacrimal ductal epithelium so far. In addition, we also tested whether the isolated and cultured ducts are suitable to study the regulation of LGDC secretion. Regulation of lacrimal gland secretion can be mediated by neurotransmitters (e.g. Ach) and growth factors (e.g. endothelial growth factor family).^[78] Activation of muscarinic receptors by Ach released from parasympathetic nerves stimulates lacrimal gland secretion. The glandular subtype of M3 muscarinic receptors have been identified in the lacrimal gland.^[79] It is more than likely that the ductal epithelia are involved in the hypersecretory effect of parasympathetic stimulation. In our study we tested the effect of carbachol on the intracellular Ca^{2+} signaling using the Ca^{2+} sensitive fluorescence dye FURA2-AM. Our results showed that carbachol dose dependently increased $[\text{Ca}^{2+}]_i$. Finally, we investigated the effects of parasympathetic stimulation on the acid/base transporters of LGDC. We found that carbachol strongly stimulates NHE activity, therefore drives Na^+ into the cell. This stimulation is followed by the activation of the AE on the basolateral membrane, which drives Cl^- into the LGDC. The Na^+ and Cl^- influx needs available H^+ and HCO_3^- inside the cell, which can come

after the dehydration of carbonic acid (H_2CO_3) by carbonic anhydrase.^[80] The stimulatory effects of carbachol on NHE and AE have been shown in the lacrimal acinar cells ^[81, 82] indicating that there must be other differences in ion transport mechanisms on the basolateral membranes between the acinar cells and LGDC. Importantly, expression of Na^+/K^+ ATPase is three to five times higher on duct cells compared to acinar cells ^[83]. Therefore, the elevated intracellular Na^+ concentration after a parasympathetic activation may stimulate the basolateral Na^+/K^+ ATPase which will increase the intracellular K^+ concentration in LGDC. Our data suggests that the Na^+/K^+ ATPase may be a crucial basolateral transporter in the mechanisms of K^+ secretion in LGDC. Following the intracellular accumulation of K^+ and Cl^- , these ions can be secreted via a coupled mechanism (K^+/Cl^- cotransporter)^[21] and/or via a separate K^+ selective cation channel ($\text{IK}_{\text{Ca}1}$ and/or BK_{Ca}) and a Cl^- selective anion channel (CFTR and/or calcium-activated chloride channel CACC, Fig. 20). Taken together, we described a lacrimal gland duct isolation technique, in which the intact ducts remain viable and in which the role of duct cells in the pre-ocular tear film secretion can be characterized. In addition we added new insights into the regulation of lacrimal gland ductal secretion. Our data and new isolation method open up the possibility to understand the physiological and pathophysiological (such as dry eye syndrome or keratoconjunctivitis sicca) roles of the lacrimal gland ductal system. Furthermore, our results may lead to the development of drugs that stimulate preocular tear secretion in patients with dry eye syndrome.

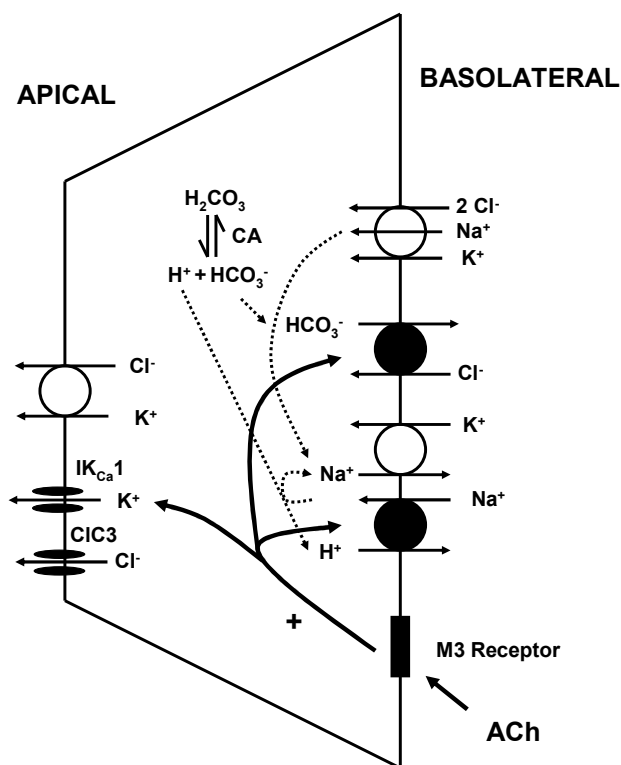


Figure 20. Model for secretion of K^+ and Cl^- by lacrimal gland ductal cells (LGDC). The model is based on the channels and transporters identified by Ubels et al.¹¹ and the functionally active acid/base transporters characterized in this study. Parasympathomimetic stimulation by carbachol strongly stimulates the NHE activity followed by the activation of AE on the basolateral membrane via Ca^{2+} signaling, which drive Na^+ and Cl^- into the LGDC. The Cl^- and Na^+ influx requires available H^+ and HCO_3^- inside the cell, generated from the dehydration of carbonic acid (H_2CO_3) by carbonic anhydrase³². The elevated intracellular Na^+ concentration can be exchanged for K^+ via the basolateral Na^+/K^+ ATPase which will increase the intracellular K^+ concentration in LGDC. The elevated intracellular Ca^{2+} concentration can also activate the $\text{IK}_{\text{Ca}1}$. CA: carbonic anhydrase, Ach: acetylcholine, CIC: chloride channel, $\text{IK}_{\text{Ca}1}$: calcium activated potassium channel.

In the second part of this thesis we utilized *in vitro* and *in vivo* experimental pancreatitis models, in which we investigated the protective role of hypersecretion and HSP72 in the course of acute pancreatitis. We also investigated the I κ B- α level to monitor the severity of the pancreatitis.

Acute pancreatitis is a common disorder that results from acute inflammatory injury of the pancreas. The pathogenesis of acute pancreatitis is not fully understood, however, a number of conditions are known to induce this disease. One of the most common etiologic factors is the ampullary obstruction resulting in bile reflux into the pancreatic ductal system. Very little is known about the role of pancreatic ductal epithelium in acute pancreatitis, however, some recent studies have suggested that HCO₃⁻ and fluid secretion by pancreatic ductal cells may represent a defence mechanism against toxic factors that can induce pancreatitis.^[30, 44] Since in previous studies it has been shown that bile acids stimulate secretion from different epithelia,^[84-87] we investigated the secretory effect of bile acids on PPDC.

First we investigated the effects of bile acids on pH_i. We chose to use the unconjugated and conjugated forms of CDC for this investigation since the majority (62%) of guinea pig bile acids is CDC^[88] and the human gallbladder bile also contains this bile acid in high concentrations.^[89] We could only estimate the concentration of bile acid that can reach the small interlobular ducts during acute biliary pancreatitis. In our experiments we used 0.1 mM as a low dose and 1 mM as a high dose of bile acids. We found that basolateral or luminal administration of CDC dose-dependently and reversibly reduced the pH_i of duct cells. However, the conjugated GCDC had a significantly smaller effect than the unconjugated CDC and notably, low concentrations of GCDC had only a very small effect on pH_i when it was administered from the luminal side. Alvaro et al. reported that 0.5 – 1.5 mM ursodeoxycholate caused a dose-dependent rapid, intracellular acidification in bile duct epithelial cells.^[90] In addition, the conjugated form of this bile acid (tauroursodeoxycholate) at 1 mM concentration had no effect on pH_i.^[90] These results are in accordance with the diffusion characteristics of bile acids. Unconjugated bile salts are weak acids and they can traverse cell membranes by passive diffusion.^[91] However, taurine or glycine conjugated bile acids are impermeable to cell membranes due to their lipid insolubility and require active transport mechanisms for cellular uptake.^[92] Recently, an increasing number of bile acid transporters have been cloned and localized to either the luminal or basolateral membranes of polarized epithelial cells.^[91, 93, 94] Basolateral administration of 1 mM CDC for 6-8 minutes damaged the membrane integrity and PPDC lost BCECF very quickly. The same concentration of CDC had no toxic effects on

the luminal membrane, however, a higher (2 mM) concentration of CDC also damaged the luminal membrane (unpublished data). In accordance with our findings, Okolo et al.^[40] also found differences between the effects of bile acids on the luminal and basolateral membranes. The basolateral membrane was much more sensitive to bile acid-induced damage (transepithelial membrane resistance decreased much more when bile acids were administered from the basolateral side) than the luminal membrane.

We next investigated the effects of bile acids on the acid/base transporters of PPDC. A high concentration of CDC strongly inhibited the NHE, NBC and AE of PPDC. This observation indicates a possible toxic effect of high doses of CDC on the activity of the acid/base transport system which was also suggested by Alvaro et al.^[90] Using 1.5 mM ursodeoxycholate, spontaneous pH_i recovery did not occur during the administration of this bile acid; however, this finding was not further investigated using the NH_4Cl pulse technique.^[90] Lower doses of ursodeoxycholate (0.5 mM) had no effect on the recovery from acid load in bile duct epithelial cells,^[90] which is in accordance with our results. Importantly, luminal administration of low doses of CDC significantly stimulated HCO_3^- efflux i.e. secretion from PPDC. It has been shown that bile acids modulate AE and CFTR in different epithelia.^[95-99] Low doses (20 μM) of taurocholic and tauro lithocholic acid augmented the stimulatory effect of secretin on HCO_3^- secretion in cholangiocytes.^[95, 96] Strazzabosco et al. also suggested that ursodeoxycholate stimulates HCO_3^- secretion in bile by a weak acid effect.^[97] Luminal administration of 0.5 mM taurocholate has been shown to stimulate a CFTR dependent electrogenic Cl^- transport in the murine distal ileum.^[99] Exposure of gastroduodenal mucosa to high concentrations of taurocholic acid was also shown to stimulate HCO_3^- secretion and therefore, can play a physiological role in the mucosal protective mechanisms.^[98] In this study, we showed that low doses of CDC selectively act on the luminal membrane to stimulate HCO_3^- secretion. Inhibition of basolateral AE and NBC by H_2DIDS and NHE by amiloride had no effect on the secretory response to CDC. However, luminal administration of H_2DIDS totally blocked the stimulated HCO_3^- efflux. Three main anion transporters/channels have been identified on the luminal membrane of PPDC namely the CFTR chloride channel, the calcium-activated chloride channel (CACC) and two members of the SLC26 family (A3 and A6) anion exchangers. Since CFTR is unaffected by H_2DIDS ,^[100] it is unlikely to be involved in the stimulatory mechanism of CDC. Taurodeoxycholate was reported to activate a chloride conductance via IP_3 -mediated Ca^{2+} signaling in the T84 colonic cell line^[84] and in cultured PDEC.^[40] Since SLC26A3 is only weakly inhibited by the disulphonic stilbene,^[101, 102] the putative anion exchanger SLC26A6

and/or the CACC are the most likely candidates for the target of CDC.^[102, 103] Most CACC are inhibited by DIDS, although human CACC in the HPAF cell line is not.^[104] Finally, we provided evidence that the stimulatory effect of low doses of luminal CDC on HCO_3^- secretion is dependent on an elevation of $[\text{Ca}^{2+}]_i$. BAPTA-AM (40 μM) slightly inhibited basal HCO_3^- secretion measured using the ammonium pulse method. In an earlier study, a lower concentration of BAPTA-AM (10 μM) had no effect on fluid secretion by guinea pig pancreatic duct cells,^[105] suggesting a dose-dependent effect of this calcium chelator. Importantly, BAPTA-AM (40 μM) totally blocked the stimulatory effect of low doses of CDC showing that this effect is Ca^{2+} dependent. However, BAPTA-AM had no effect on the inhibitory action of high doses of basolateral CDC on HCO_3^- secretion indicating that a Ca^{2+} independent mechanism is responsible for this effect. Our results suggest that the pancreatic ductal epithelium is remarkably resistant to attack by the conjugated bile salt GCDC, which is the major bile salt in the guinea pig's gall bladder. Whilst GCDC decreased pH_i and elevated $[\text{Ca}^{2+}]_i$ it had no detectable effect on HCO_3^- secretion. In contrast, the unconjugated CDC caused marked changes in pH_i and $[\text{Ca}^{2+}]_i$ and, depending on the dose, either stimulated or inhibited HCO_3^- secretion. Although, it has been shown that the triggering mechanisms of intracellular protease activation do not require bile influx into the pancreatic ductal tree,^[106-108] a flow of bile into the pancreatic ductal system may occur after the first 24 to 48 h.^[109, 110] Theoretically, when small stones obstruct the pancreatic duct and the 'common channel' is formed,^[111] by the pancreatic and bile duct, bile acids start diffusing up into the ductal tree and reach the interlobular ducts in a low concentration, ductal cells may try to wash out the toxic acids and thus defend the acinar cells. The subsequent bile acid-induced stimulated HCO_3^- and fluid secretion may protect the pancreas in different ways. Firstly, the elevated luminal pressure stops or delays the bile acid diffusion towards the acinar tissue. Importantly, the higher ductal pressure may push the small stones through the papilla and open the way for the pancreatic and bile fluid. However, if this defense mechanism is not sufficient and the bile concentration rises further, thus leading to damage the epithelial barrier, the secretory mechanisms of pancreatic ductal cells are blocked and the ducts can no longer act as a defensive wall against the toxic bile. On the other hand, high concentrations of bile acids reaching the pancreatic ductal cells from the basolateral side (either from the blood and/or from the lumen due to the damage of the ductal barrier) inhibit HCO_3^- and fluid secretion, therefore, may contribute to the progression of acute pancreatitis. We postulate that these contrasting effects of bile acids may have an important role in the pathogenesis of bile-induced pancreatitis.

Another non-alcoholic etiologic factor which may play role during acute pancreatitis is hyperlipidemia. A hyperlipidemia prevalence of 12-38% has been reported in acute human pancreatitis in previous studies.^[112-114] Even though a few animal studies have been published in this topic, the results are fairly contradictory,^[115-118] therefore, the role of hyperlipidemia in acute pancreatitis is still debated. Hyperlipidemia has been shown to attenuate heat shock protein expression in the heart.^[47] Although, it was not known whether hyperlipidemia leads to a decreased heat shock response in the pancreas, it was tempting to speculate that this mechanism is involved in the increased severity of pancreatitis in hyperlipidemia. Accordingly, we measured the pancreatic HSP72 production. Pancreatic HSP72 was induced by acute necrotizing pancreatitis using high doses of Arg^[119] in animals on the high-cholesterol diet and in others on the normal diet. We found that the expression of HSP72 did not differ between the two groups. In addition we determined the pancreatic I κ B- α levels and found that I κ B- α expression was unaltered by cholesterol treatment. However, in the rats with acute necrotizing pancreatitis the high-cholesterol diet significantly decreased the expression of I κ B- α as compared those receiving the normal diet.

In summary, we tried to provide a better insight into epithelial cell physiology under normal and pathophysiological conditions. Our results may represent a possible aid in the treatment of different diseases by contributing to the better understanding of epithelial cell function.

5. ACKNOWLEDGEMENTS

I would like to thank all of the people who have helped and inspired me during my doctoral study.

I am grateful to **Prof. Dr. János Lonovics** and **Prof. Dr. Tibor Wittman** past and present head of the First Department of Medicine, who gave me the opportunity to work in the department.

My warm thanks are due to **Prof. Tamás Takács**, who provided me the opportunity to start my Ph.D. in his scientific team. I am indeed grateful for his valuable advice and help.

I would like to express my deep and sincere gratitude to my supervisors **Dr. Péter Hegyi** and **Dr. Zoltán Rakonczay Jr.** Their wide knowledge and their logical way of thinking have been of great value for me. Their understanding and encouragement provided a good basis for the present thesis.

I wish to thank **Prof. Barry E. Argent** and **Dr. Mike A. Gray**, our collaborators from the University of Newcastle, UK for their extensive discussions of my work and interesting explorations.

I would also like to thank my colleagues and friends, **Béla Ózsvári**, **Imre Ignáth**, **József Maléth** and **Lajos Nagy** for all the emotional support, entertainment, and care they provided.

This work would not have been possible to accomplish without the assistance of **Zoltánné Fuksz**, **Edit Magyarné Pálfi**, **Ágnes Sitkei**, **Miklósné Árva**.

We are grateful to **Prof. András Varró**, the Head of Department of Pharmacology and Pharmacotherapy, who provided us the opportunity to work in his department .

This work was supported by Hungarian Scientific Research Fund grants to J.L. (T43066) and to Z.R. (PF6395), Bolyai Postdoctoral Fellowships to P.H. (00276/04) and to Z.R. (00218/06),

KPI Research Grant to A.V. (KPI/BIO-37), Joint International Grant (HAS and the Royal Society) to P.H and M.A.G, Asboth Grant to J.L. (XTPPSRT1), Hungarian Medical Research Council grant to J.L. (517/2006), and The Physiological Society Junior Fellowship to Z.R..

My deepest gratitude goes to **my family** for their unflagging love and support throughout my life; this dissertation would have been impossible to accomplish without their help. I dedicate this thesis to them.

6. REFERENCES

1. Argent BE, Gray MA. Regulation and formation of fluid and electrolyte secretions by pancreatic ductal epithelium. In: *Biliary and Pancreatic Ductal Epithelia. Pathobiology and Pathophysiology*, edited by Sirica AE and Longnecker DS. New York: Dekker, 1997, p. 349–377.
2. Bartle HJ, Harkins MJ. The gastric secretion: its bactericidal value to man. *Amer J Med Sci* 1925;**169**:373-388.
3. Gianella RA, Broitman SA, Zamcheck N. Gastric acid barrier to ingested microorganisms in man: Studies in vivo and in vitro. *Gut* 1972;**13**:251-256.
4. Bockman D. Anatomy and fine structure. In: Beger HG, Buchler M, Kozarek R, eds. *The Pancreas: An Integrated Textbook of Basic Science, Medicine and Surgery*. 2008. *In press*.
5. Martin CL, Munnell J, Kaswan R. Normal ultrastructure and histochemical characteristics of canine lacrimal glands. *Am J Vet Res* 1988;**49**:1566-72.
6. Millar TJ, Herok G, Koutavas H, et al. Immunohistochemical and histochemical characterisation of epithelial cells of rabbit lacrimal glands in tissue sections and cell cultures. *Tissue Cell* 1996;**28**:301-12.
7. M. Cerejido, RG Contreras, MR Garcia, et al. Epithelial polarity. In: NK Wills, L Reuss and SA Lewis, eds. *Epithelial transport: A guide to Methods and Experimental Analysis*. 1996.
8. Beltinger J, Hildebrand P, Drewe J, et al. Effect of spiroglumide, a gastrin receptor antagonist, on acid secretion in humans. *Eur J Clin Invest* 1999;**29**:153-59.
9. Kovacs TO, Walsch JH, Maxwell J, et al. Gastrin is a major regulator of the gastric acid secretion in dogs: proof by monoclonal antibody neutralization. *Gastroenterology* 1989;**97**:1406-13.
10. Hersey SJ, Sachs G. Gastric acid secretion. *Physiol Rev* 1995;**75**:155-89.
11. Soll AH. The interaction of histamine with gastrin and carbamylcholine on oxygen uptake by isolated mammalian parietal cells. *J Clin Invest* 1978;**61**:381-9.
12. Black JW, Shankley NP. How does gastrin act on stimulate oxyntic cell secretion. *TIPS* 1987;**8**:486-90.

13. Koh TJ, Goldenring JR, Ito S, et al. Gastrin deficiency results in altered gastric differentiation and decreased colonic proliferation in mice. *Gastroenterology* 1997;**113**:1015-25.
14. Friis-Hansen L, Sundler F, Li Y, et al. Impaired gastric acid secretion in gastrin-deficient mice. *Am J Physiol* 1998;**274**:G561-8.
15. Chen D, Zao CM, Dockray GJ, et al. Glycine-extended gastrin synergizes with gastrin 17 to stimulate acid secretion in gastrin-deficient mice. *Gastroenterology* 2000;**119**:756-65.
16. Hemady R, Chu W, Foster CS. Keratoconjunctivitis sicca and corneal ulcers. *Cornea* 1990;**9**:170-3.
17. Golubovic S, Parunovic A. Corneal perforation in dry eye patients. *Fortschr Ophthalmol* 1987;**84**:33-7.
18. Rios JD, Ferdman D, Tepavcevic V, et al. Role of Ca^{2+} and protein kinase C in cholinergic, and alpha1-adrenergic agonists and EGF stimulated mitogen-activated protein kinase activity in lacrimal gland. *Adv Exp Med Biol* 2002;**506**:185-90.
19. Walcott B, Birzgalis A, Moore LC, et al. Fluid secretion and the Na^{+} - K^{+} -2Cl⁻ cotransporter in mouse exorbital lacrimal gland. *Am J Physiol Cell Physiol*. 2005;**289**:C860-7.
20. Saito Y, and Kuwahara S. Effect of acetylcholine on the membrane conductance of the intralobular duct cells of the rat exorbital lacrimal gland. *Adv Exp Med Biol* 1994;**350**:87-92.
21. Ubels JL, Hoffman HM, Srikanth S, et al. Gene expression in rat lacrimal gland duct cells collected using laser capture microdissection: evidence for K^{+} secretion by duct cells. *Invest Ophthalmol Vis Sci* 2006;**47**:1876-85.
22. Dobosz M, Hac S, Mionskowska L, et al. Organ Microcirculatory Disturbances in Experimental Acute Pancreatitis. A Role of Nitric Oxide. *Physiol Res* 2005;**54**:363-8.
23. Warzecha Z, Dembiński A, Ceranowicz P, et al. Deleterious effect of Helicobacter pylori infection on the course of acute pancreatitis in rats. *Pancreatology* 2002;**2**:386-95.
24. Case RM, Hotz J, Hutson D, et al. Electrolyte secretion by the isolated cat pancreas during replacement of extracellular bicarbonate by organic anions and chloride by inorganic anions. *Journal of Physiology* 1979;**286**:563-76.
25. Noviak I, Greger R. Properties of the luminal membrane of isolated perfused rat pancreatic ducts: effect of cyclic AMP and blockers of chloride transport. *Pflügers Archiv* 1988;**411**:546-53.
26. Zhao H, Star RA, Muallem S. A Membrane localization of H^{+} and HCO_3^{-} transporters in the rat pancreatic duct. *Journal of General Physiology* 1994;**104**:57-85.

27. Sewell WA, Young JA. Secretion of electrolytes by the pancreas of the anaesthetized rat. *Journal of Physiology* 1975;**252**:379-96.
28. Yamamoto A, Ishiguro H, Ko SBH, et al. Ethanol induces fluid hypersecretion from guinea-pig pancreatic duct cells. *J Physiol* 2003;**551.3**:917-26.
29. Yamamoto M, Shirohara H, Otsuki M. CCK-, secretin-, and cholinergic-independent pancreatic fluid hypersecretion in protease inhibitor-treated rats *Am J Physiol Gastrointest Liver Physiol* 1998;**274**: G406-12.
30. Hegyi P, Ördögh B, Rakonczai Z, et al. Effect of herpesvirus infection on pancreatic duct cell secretion. *World J Gastroenterol* 2006;**11**:5997-6002.
31. Opie EL. The etiology of acute haemorrhagic pancreatitis. *Johns Hopkins Hospital Bulletin* 1901;**12**:182-8.
32. Niederau C, Niedereu M, Luthen R, et al. Pancreatic exocrine secretion in acute experimental pancreatitis. *Gastroenterology* 1990;**99**:1120-7.
33. Senninger N. Bile-induced pancreatitis. *Eur Surg Res* 1992;**24**:68-73.
34. Pandol SJ, Saluja AK, Imrie CW, et al. Acute pancreatitis bench to the bedside. *Gastroenterology* 2007;**132**:1127-51.
35. Voronina S, Longbottom R, Sutton R, et al. Bile acids induce calcium signals in mouse pancreatic acinar cells: implications for bile-induced pancreatic pathology. *J Physiol* 2002;**540**:49-55.
36. Fischer L, Gukovskaya AS, Penninger JM, et al. Phosphatidylinositol 3-kinase facilitates bile acid-induced Ca^{2+} responses in pancreatic acinar cells. *Am J Physiol Gastrointest Liver Physiol* 2007;**292**:G875-86.
37. Raraty M, Ward J, Erdemli G, et al. Calcium-dependent enzyme activation and vacuole formation in the apical granular region of pancreatic acinar cells. *Proc Natl Acad Sci USA* 2000;**97**:13126-31.
38. Kim JY, Kim KH, Lee JA, et al. Transporter-mediated bile acid uptake causes Ca^{2+} -dependent cell death in rat pancreatic acinar cells. *Gastroenterology* 2002;**122**:1941-53.
39. Farmer RC, Tweedie J, Maslin S, et al. Effects of bile salts on permeability and morphology of main pancreatic duct in cats. *Dig Dis Sci* 1984;**29**:740-51.
40. Okolo C, Wong T, Moody MW, et al. Effect of bile acids on dog pancreatic duct epithelial cell secretion and monolayer resistance. *Am J Physiol Gastrointest Liver Physiol* 2002;**283**:G1042-50.
41. Reber HA, Mosley JG. The effect of bile salt on the pancreatic duct mucosal barrier. *Br J Surg* 1980;**67**:59-62.

42. Hegyi P, Rakonczay Z Jr, Tiszlavicz A, et al. SLC26 transporters and the inhibitory control of pancreatic ductal bicarbonate secretion. In: Novartis symposia series, Novartis Found Symp. No. 273. John Wiley & Sons, London 2006; 73:164-73; discussion 173-6, 261-4.
43. Hegyi P, Rakonczay Z Jr. The inhibitory pathways of pancreatic ductal bicarbonate secretion. *Intl J Biochem Cell Biol* 2007;**39**:25-30.
44. Czako L, Yamamoto M, Otsuki M. Exocrine pancreatic function in rats after acute pancreatitis. *Pancreas* 1997;**15**:83-90.
45. Argent BE, Case RM. Pancreatic ducts. Cellular mechanism and control of bicarbonate secretion. In: Physiology of the Gastrointestinal Tract. New York: Raven Press 1994:1473-97.
46. Dominguez-Munoz JE, Malfertheiner P, Ditschuneit HH, et al. Hyperlipidemia in acute pancreatitis. Relationship with etiology, onset, and severity of the disease. *Int J Pancreatol* 1991;**10**:261-7.
47. Csont T, Balogh G, Csonka C, et al. Hyperlipidemia induced by high cholesterol diet inhibits heat shock response in rat hearts. *Biochem Biophys Res Commun* 2002;**290**:1535-38.
48. Wilson SH, Caplice NM, Simari RD et al. Activated nuclear factor-kappa B is present in the coronary vasculature in experimental hypercholesterolemia. *Atherosclerosis* 2000;**148**:23-30.
49. Rakonczay Jr Z, Jármay K, Kaszaki J, et al. NF- κ B activation is detrimental in arginine-induced acute pancreatitis. *Free Radic Biol Med* 2003;**34**:696-709.
50. Rakonczay Jr Z, Takács T, Boros I, et al. Heat shock proteins and the pancreas. *J Cell Physiol* 2003;**195**:383-91.
51. Verma IM. Nuclear factor (NF)- κ B proteins: therapeutic targets. *Ann Rheum Dis* 2004;**63**:57-61.
52. Hegyi P, Rakonczay Z Jr, Sari R et al. L-arginine induced experimental pancreatitis. Review. *World J Gastroenterol* 2004;**10**:2003-9.
53. Hegyi P, Takacs T, Jarmay K, et al. Spontaneous and cholecystokinin-octapeptide-promoted regeneration of the pancreas following L-arginine-induced pancreatitis in rat. *Int J Pancreatol* 1997;**22**:193-200.
54. Czakó L, Takács T, Varga IS, et al. Involvement of oxygen-derived free radicals in L-arginine-induced acute pancreatitis. *Dig Dis Sci* 1998;**43**:1770-7.
55. Hegyi P, Rakonczay Z Jr, Sari R, et al. Insulin is necessary for the hypertrophic effect of CCK-8 following acute necrotizing experimental pancreatitis. *World J Gastroenterol* 2004;**10**:2275-7.

56. Hegyi P, Czako L, Takacs T, et al. Pancreatic secretory responses in L-arginine-induced pancreatitis: comparison of diabetic and nondiabetic rats. *Pancreas* 1999;**19**:167-74.
57. Berglindh T, Obrink KJ. A method for preparing isolated glands from the rabbit gastric mucosa. *Acta Physiol Scand* 1976;**96**:150-9
58. Booth C, Patel S, Bennion GR, et al. The isolation and culture of adult mouse colonic epithelium. *Epithelial Cell Biol* 1995;**4**:76-86.
59. Argent BE, Arkle S, Cullen MJ, et al. Morphological, biochemical and secretory studies on rat pancreatic ducts maintained in tissue culture. *Q J Exp Physiol* 1986;**71**:633-48.
60. Hegyi P, Rakonczay Z Jr, Gray MA, et al. Measurement of intracellular pH in pancreatic duct cells. A new method to calibrating the fluorescence data. *Pancreas* 2004;**28**:427-34.
61. Thomas JA, Buchsbaum RN, Zimniak A, et al. Intracellular pH-measurements in Ehrlich ascites tumor cells utilizing spectroscopic probes generated in situ. *Biochemistry* 1979;**18**:2210-18.
62. Ishiguro H, Steward MC, Lindsay ARG, et al. Accumulation of intracellular HCO_3^- by Na^+ - HCO_3^- cotransport in interlobular ducts from guinea-pig pancreas. *J Physiol* 1996;**495**:169-78.
63. Hegyi P, Gray MA, Argent BE. Substance P inhibits bicarbonate secretion from guinea-pig pancreatic ducts by modulating an anion exchanger. *Am J Physiol Cell Physiol* 2003;**285**:C268-76.
64. Szalmay G, Varga G, Kajiyama F, et al. Bicarbonate and fluid secretion by cholecystokinin, bombesin and acetylcholine in isolated guinea-pig pancreatic ducts. *J Physiol* 2001;**535**:795-807.
65. Weintraub WH, Machen TE. pH regulation in hepatoma cells: roles for Na-H exchange, Cl- HCO_3^- exchange, and Na- HCO_3^- cotransport. *Am J Physiol Gastrointest Liver Physiol* 1989;**257**:G317-27.
66. Giricz Z, Csonka C, Onody A et al. Role of cholesterol-enriched diet and the mevalonate pathway in cardiac nitric oxide synthesis. *Basic Res Cardiol* 2003;**98**:304–10.
67. Hodges RR, Dartt DA. Regulatory pathways in lacrimal gland epithelium. *Int Rev Cytol.* 2003;**231**:129-96.
68. Hegyi P, Rakonczay Z Jr, Tizslavicz L, et al. Protein kinase C mediates the inhibitory effect of substance P on bicarbonate secretion from guinea pig pancreatic ducts. *Am J Physiol Cell Physiol* 2005;**288**:C1030-41.
69. Botelho SY, Martinez EV. Electrolytes in lacrimal gland fluid and in tears at various flow rates in the rabbit. *Am J Physiol* 1973;**225**:606-9.

70. Alexander JH, van Lennep EW, Young JA. Water and electrolyte secretion by the exorbital lacrimal gland of the rat studied by micropuncture and catheterization techniques. *Pflugers Arch* 1972;**337**:299-309.
71. Walcott B, Birzgalis A, Moore LC, et al. Fluid secretion and the $\text{Na}^+\text{-K}^+\text{-2Cl}^-$ cotransporter in mouse exorbital lacrimal gland. *Am J Physiol Cell Physiol* 2005;**289**:C860-7.
72. Koyama K, Sasaki I, Naito H, et al. Induction of epithelial Na^+ channel in rat ileum after proctocolectomy. *Am J Physiol* 1999;**276**:G975-84.
73. Romero JR, Rivera A, Lanca V, et al. $\text{Na}^+/\text{Ca}^{2+}$ exchanger activity modulates connective tissue growth factor mRNA expression in transforming growth factor beta1- and Des-Arg10-kallidin-stimulated myofibroblasts. *J Biol Chem* 2005;**15**;280:14378-84.
74. Kiela PR, Ghishan FK. $\text{Na}^+\text{-H}^+$ exchange in mammalian digestive tract. *Physiology of the gastrointestinal tract*. 4th ed. Edited by Johnson LR., USA, Elsevier Academic Press; 2006:1847-81.
75. Soleimani M, Burnham CE. $\text{Na}^+:\text{HCO}_3^-$ cotransporters (NBC): cloning and characterization. *J Membr Biol* 2001;**183**:71-84.
76. Alper SL. The band 3-related anion exchanger (AE) gene family. *Annu Rev Physiol* 1991;**53**:549-64.
77. Ko SB, Luo X, Hager H, et al. AE4 is a DIDS-sensitive $\text{Cl}^-/\text{HCO}_3^-$ exchanger in the basolateral membrane of the renal CCD and the SMG duct. *Am J Physiol Cell Physiol* 2002;**283**:C1206-18.
78. Dartt DA. Regulation of lacrimal gland secretion by neurotransmitters and the EGF family of growth factors. *Exp Eye Res* 2001;**73**:741-52.
79. Mauduit P, Jammes H, Rossignol B. M3 muscarinic acetylcholine receptor coupling to PLC in rat exorbital lacrimal acinar cells. *Am J Physiol Cell Physiol* 1993;**264**:C1550-60.
80. Ogawa Y, Toyosawa S, Inagaki T, et al. Carbonic anhydrase isozyme VI in rat lacrimal gland. *Histochem Cell Biol* 1995;**103**:387-94.
81. Lambert RW, Maves CA, Mircheff AK. Carbachol-induced increase of Na^+/H^+ antiport and recruitment of $\text{Na}^+,\text{K}^+\text{-ATPase}$ in rabbit lacrimal acini. *Curr Eye Res* 1993;**12**:539-51.
82. Lambert RW, Bradley ME, Mircheff AK. pH-sensitive anion exchanger in rat lacrimal acinar cells. *Am J Physiol* 1991;**260**:G517-23.
83. Okami T, Yamamoto A, Takada T. Ultrastructural localization of $\text{Na}^+,\text{K}^+\text{-ATPase}$ in the exorbital lacrimal gland of rat. *Invest Ophthalmol Vis Sci* 1992;**33**:196-204.

84. Devor DC, Sekar MC, Frizzell RA, et al. Taurodeoxycholate activates potassium and chloride conductances via an IP₃-mediated release of calcium from intracellular stores in a colonic cell line (T84). *J Clin Invest* 1993;**92**:2173–81.
85. Dharmasathaphorn K, Huott PA, Vongkovit P, et al. Cl⁻ secretion induced by bile salts. A study of the mechanism of action based on a cultured colonic epithelial cell line. *J Clin Invest* 1989;**84**: 945–53.
86. Freel RW. Dihydroxy bile salt-induced secretion of rubidium ion across the rabbit distal colon. *Am J Physiol Gastrointest Liver Physiol* 1987;**252**:G554–61.
87. Freel RW, Hatch M, Earnest DL, et al. Dihydroxy bile salt-induced alterations in NaCl transport across the rabbit colon. *Am J Physiol Gastrointest Liver Physiol* 1983;**245**: G808–G815.
88. Ting GS, Xu GR, Batta AK, et al. Ursodeoxycholic acid, chenodeoxycholic acid, and 7-ketolithocholic acid are primary bile acids of the guinea pig. *J Lipid Res* 1990;**31**:1301-6.
89. Berr F, Stellaard F, Pratschke E, et al. Effects of cholecystectomy on the kinetics of primary and secondary bile acids. *J Clin Invest* 1989;**83**:1541-50.
90. Alvaro D, Mennone A, Boyer JL. Effect of ursodeoxycholic acid on intracellular pH regulation in isolated rat bile duct epithelial cells. *Am J Physiol Gastrointest Liver Physiol* 1993;**28**:G783-91.
91. Trauner M., Boyer JL. Bile salt transporters: Molecular characterization, function, and regulation. *Physiol Rev* 2003;**83**:633-71.
92. Meier PJ. Molecular mechanisms of hepatic bile salt transport from sinusoidal blood into bile. *Am J Physiol Gastrointest Liver Physiol* 1995;**269**:G801-12.
93. Hagenbuch B, Stieger B, Foguet M, et al. Functional expression cloning and characterization of the hepatocyte Na-bile acid cotransport system. *Proc Natl Acad Sci USA* 1991;**88**:10629-33.
94. Lazaridis KN, Pham L, Tietz P, et al. Rat cholangiocytes absorb bile acids at their apical domain via the ileal sodium-dependent bile acid transporter. *J Clin Invest* 1997;**100**:2714-21.
95. Alpini G, Glaser S, Robertson W, et al. Bile acids stimulate proliferative and secretory events in large but not small cholangiocytes. *Am J Physiol Gastrointest Liver Physiol* 1997;**36**:G518-29.
96. Alpini G, Glaser S, Ueno Y, et al. Bile acid feeding induces cholangiocyte proliferation and secretion: evidence for bile acid-regulated ductal secretion. *Gastroenterology* 1999;**116**:179-86.

97. Strazzabosco M, Sakisaka S, Hayakawa T, et al. Effect of UDCA on intracellular and biliary pH in isolated rat hepatocyte couplets and perfused livers. *Am J Physiol Gastrointest Liver Physiol* 1991;**26**:G58-69.
98. Konturek SJ, Bilski J, Tasler J, et al. Gastroduodenal alkaline response to acid and taurocholate in conscious dogs. *Am J Physiol Gastrointest Liver Physiol* 1984;**247**:G149-54.
99. Bijvelds MJ, Jorna H, Verkade HJ, et al. Activation of CFTR by ASBT-mediated bile salt absorption. *Am J Physiol Gastrointest Liver Physiol* 2005;**289**:G870-9.
100. Paradiso AM, Ribeiro CMP, Boucher RC. Polarized signaling via purinoceptors in normal and cystic fibrosis airway epithelia. *J Gen Physiol* 2001;**117**:53-68.
101. Chernova MN, Jiang LW, Shmukler BE, et al. Acute regulation of the SLC26A3 congenital chloride diarrhoea anion exchanger (DRA) expressed in *Xenopus* oocytes. *J Physiol* 2003;**549**:3-19.
102. Ko SBH, Shcheynikov N, Choi JY, et al. A molecular mechanism for aberrant CFTR-dependent HCO₃⁻ transport in cystic fibrosis. *EMBO J* 2002;**21**:5662-72.
103. Wang Z, Petrovic S, Mann E, et al. Identification of an apical Cl⁻/HCO₃⁻ exchanger in the small intestine. *Am J Physiol Gastrointest Liver Physiol* 2002;**282**:G573-9.
104. Winpenny JP, Harris A, Hollingsworth MA, et al. Calcium-activated chloride conductance in a pancreatic adenocarcinoma cell line of ductal origin (HPAF) and in freshly isolated human pancreatic duct cells. *Pflügers Arch-Eur J Physiol* 1998;**435**:796-803.
105. Yamamoto A, Ishiguro H, Shigeru BHK, et al. Ethanol induces fluid hypersecretion from guinea-pig pancreatic duct cells. *J Physiol* 2003;**551**:917-26.
106. DiMagno EP, Shorter RG, Taylor WF, et al. Relationships between pancreaticobiliary ductal anatomy and pancreatic ductal and parenchymal histology. *Cancer* 1982;**49**:361-8.
107. Lerch MM, Hernandez CA, Adler G. Gallstones and acute pancreatitis--mechanisms and mechanics. *Dig Dis Sci* 1994;**12**:242-7.
108. Lerch MM, Weidenbach H, Hernandez CA, et al. Pancreatic outflow obstruction as the critical event for human gall stone induced pancreatitis. *Gut* 1994;**35**:1501-3.
109. Lerch MM, Saluja AK, Dawra R, et al. Acute necrotizing pancreatitis in the opossum: earliest morphological changes involve acinar cells. *Gastroenterology* 1992;**103**:205-13.
110. Lerch MM, Saluja AK, Runzi M, et al. Pancreatic duct obstruction triggers acute necrotizing pancreatitis in the opossum. *Gastroenterology* 1993;**104**:853-61.
111. Lerch MM. Clinical Course and Treatment Principles of Biliary Acute Pancreatitis. In: Beger HG, Buchler M, Kozarek R, eds. *The Pancreas: An Integrated Textbook of Basic Science, Medicine and Surgery*. 2008. *In press*.

112. Dominguez-Munoz JE, Malfertheiner P, Ditschuneit HH, et al. Hyperlipidemia in acute pancreatitis. Relationship with etiology, onset, and severity of the disease. *Int J Pancreatol* 1991;**10**:261-67.
113. Toskes PP. Hyperlipidemic pancreatitis. *Gastroenterol Clin North Am* 1990;**19**:783-91.
114. Yadav D, Pitchumoni CS. Issues in hyperlipidemic pancreatitis. *J Clin Gastroenterol* 2003;**36**:54-62.
115. Hofbauer B, Friess H, Weber A. Hyperlipaemia intensifies the course of acute oedematous and acute necrotising pancreatitis in the rat. *Gut* 1996;**38**:753-58.
116. Saharia P, Margolis S, Zuidema GD, et al. Acute pancreatitis with hyperlipemia: studies with an isolated perfused canine pancreas. *Surgery* 1997;**82**:60-67.
117. Kimura W, Mossner J. Role of hypertriglyceridemia in the pathogenesis of experimental acute pancreatitis in rats. *Int. J Pancreatol* 1996;**20**:177-84.
118. Paye F, Chariot J, Molas G, et al. Release of nonesterified fatty acids during cerulein-induced pancreatitis in rats. *Dig Dis Sci* 1996;**41**:1959-65.
119. Hegyi P, Takacs T, Tiszlavicz L, et al. Recovery of exocrine pancreas six months following pancreatitis induction with L-arginine in streptozotocin-diabetic rats. *J Physiol Paris* 2000; **94**:51-5.

7. ANNEX